Transport in Porous Media **52:** 229–266, 2003.

WAG Displacements of Oil-Condensates Accounting for Hydrocarbon Ganglia

PAVEL BEDRIKOVETSKY
State North Fluminense University/Petrobras, Rod. Amaral Peixoto Km 163, Imboacica, Macaé 27925-310, Rio de Janeiro, Brazil

(Received: 22 August 2002)

Abstract. During two-phase flow in porous media, non-wetting phase is present simultaneously in states of mobile connected continuum and of trapped isolated ganglia. Mass exchange between these two parts of non-wetting phase is going on by dissolution and diffusion of component in the wetting phase, so, compositions of non-wetting phase in both parts are different. Nevertheless, the traditional mathematical model for two-phase multicomponent transport in porous media assumes the homogeneous distribution of each component in the overall non-wetting phase. New governing equations honouring ganglia of non-wetting phase are derived. They are successfully verified by a number of laboratory tests. Analytical model is developed for miscible water-alternate-gas (WAG) displacement of oil-condensates. The modelling shows that the significant amount of oil-condensate is left in porous media after miscible WAG, while the traditional model predicts that the miscible displacement results in the total sweep.

Key words: oil, condensate, EOR, WAG, ganglia, residual oil, wettability.

Nomenclature

c	gas concentration in active oleic phase.
D	3-D domain of flow.
f	fractional flow for oleic phase (gas-condensate, gas).
k_{r}	relative phase permeabilities.
O	initial of coordinates on the plane (s, f).
O_{I}, O_{J}	points on the (s,f) plane which correspond to velocities of concentration fronts.
p	pressure.
q	volume (mass) exchange between active phase and ganglia.
q_{c}	volume (mass) exchange by gas component between active phase and ganglia.
$q_{1-\mathrm{c}}$	volume (mass) exchange by oil-condensate component between active phase and ganglia.
s	saturation of overall oleic phase which is just called saturation throughout this paper.
s^0	maximum saturation during waterflooding.
s_{g}	minimum saturation at which ganglia saturation becomes zero.
s_{or}	saturation of oil-condensate which resides in porous media after waterflooding (gas-condensate residual).
t, T	dimensional and dimensionless time.
u	dimensionless velocity of the total flux.
u_{W}, u_{O}	phase velocities.

U	velocity of the total two-phase flux.
V_{c}	velocity of concentration front.
V_{s}	velocity of the displacement (saturation) front.
x, X	dimensional and dimensionless linear coordinate.

Subscripts and Superscripts

a	relates to the active phase.
I	initial (saturation, concentration).
J	injected (fractional flow, concentration).
m	mass (flux, concentration, etc.).
O, G	oil-condensate and gas components.
t	relates to the trapped phase (ganglia).
W, O	for water and oleic phases.
0	boundary value on the injector (flux, concentration).
$+$	value ahead of the shock front.
$-$	value behind the shock front.

Greek Symbols

λ	total mobility of two phases.
μ	viscosity.
ξ	self-similar coordinate which equals to X/T.
ρ	density.
Γ^{+}, Γ	surfaces of injection and of production.
Φ	porosity.
Ω	arbitrary reference volume.

1. Introduction

Maintenance pressure development of gas-condensate fields by gas injection is an effective method of improved gas-condensate recovery. Pressure maintenance above the dew point allows preventing liquid condensate precipitation and provides high displacement efficiency. Nevertheless, highly mobile gas will finger through reservoir fluid, leading to early breakthrough and low sweep efficiency.

Injection of water in gas-condensate reservoir will not result in viscous fingering. Nevertheless, high gas saturation resides after displacement of gas phase by water. Pressure maintenance in gas-condensate fields by injection of water have been proposed and studied (Hawes *et al.*, 1986; Fishlock *et al.*, 1988; Carson, 1989; Henderson *et al.*, 1991a, b).

The WAG process (Water Alternate Gas), which is a combination of gas and water floods, have also been studied in gas-condensate recovery both theoretically and experimentally (Caudle and Dyes, 1958; Lake, 1989; Bedrikovetsky, 1993; Cullick *et al.*, 1993). Compared with gas injection, fingering is suppressed by the simultaneous injection of water, since this reduces the apparent mobility contrast between the injected and displaced fluids (Lake, 1989; Blunt and Christie, 1993).

The WAG process in gas-condensate fields is described by the basic equations for two-phase multicomponent transport in porous media. This model contains phase saturations and concentration of each component in each phase (Aziz and Settari, 1979; Lake, 1989; Bedrikovetsky, 1993; Green and Willhite, 1998). It means that the model assumes the homogeneity of distribution of components in each phase. The consequence is zero residual gas-condensate saturation after miscible displacement by gas at mobile water presence. The same schema is valid for residual oil after miscible WAG displacements.

Nevertheless, non-wetting phase is present in porous media as a continuous phase and also as separated ganglia and droplets (Stalkup, 1983; Barenblatt and Entov, 1972; Chartsis *et al.*, 1983; Barenblatt *et al.*, 1987; Lake, 1989; Nikolaevskii, 1993). If the component is soluble in non-wetting phase and is insoluble in wetting phase, it cannot freely diffuse between the continuous part of non-wetting phase and the ganglia of non-wetting phase. Therefore, concentrations of this component in the continuous part and in the ganglia of the non-wetting phase are different. Therefore, the basic equations for two-phase multicomponent transport in porous media are to be modified.

The separation of non-wetting phase on continuous part and on ganglia was observed during the laboratory displacement under a microscope and by the network micro modelling of two-phase displacements (Chartsis *et al.*, 1983; Campbell and Orr, 1985; Dullien, 1992; Stauffer and Aharony, 1992; Seljakov and Kadet, 1997). Literature reports of laboratory miscible WAG floods clearly indicate that the presence of water at high saturations blocks oil from contact with an injection solvent (Raimondi and Torcaso, 1964; Stalkup, 1970; Shelton and Schneider, 1975; Tiffin *et al.*, 1991; Green and Willhite, 1998).

The division of the overall phase saturation on the continuous part and on the separated part has been proposed in the literature. A ganglia saturation as a function of overall non-wetting phase saturation (so called water blocking function) has been obtained from laboratory displacements (Raimondi and Torcaso, 1964; Stalkup, 1970; Shelton and Schneider, 1975; Tiffin and Yellig, 1983; Tiffin *et al.*, 1991), and correlation expressions have been developed (Raimondi and Torcaso, 1964; Green and Willhite, 1998). It was already shown how to calculate water blocking function from hysteretic relative phase permeability for non-wetting phase (Lake, 1989).

Equations for immiscible displacement honouring discontinuity of one phase have been derived (Carson, 1989), and they coincide with the traditional Rapoport-Leas model.

In the current paper we derive equations for two-phase transport of multicomponent fluids honouring phase discontinuities. The equations derived differ significantly from the traditional model, which assume the homogeneous distribution of components in each phase. The model derived has a hysteretic behaviour such that the system of governing equations and formulation of initial and boundary value problems are different for imbibition and for drainage.

The model has been successfully verified by comparison with a number of laboratory experiments.

Analytical solutions for one-dimensional miscible WAG displacement have been obtained. The solutions show that a significant amount of gas-condensate is left in porous media after the displacement in ganglia state, while the traditional model gives the total sweep of gas-condensate after miscible displacement. The model developed is applicable to miscible WAG injection in oil reservoirs.

2. Formulation of the Phenomenon

After displacement of gas-condensate by water in water-wet porous media the residual gas-condensate forms separated ganglia and droplets (Aziz and Settari, 1979; Lake, 1989; Bedrikovetsky, 1993) (Figure 1(a)). Capillary forces equilibrate pressure gradient on an isolated ganglia, therefore, ganglia are immobile. The mobile part of non-wetting phase is geometrically connected (Figure 1(b)). So, non-wetting oleic phase is present in porous media in connected mobile state (active phase) and as separated ganglia (trapped phase). Both parts of non-wetting phase are isolated from each other by water.

Under the strong domination of capillary forces over viscous forces the phases are distributed over the porous space according to wettability. The placing of active and trapped parts of non-wetting phase and of water on micro level is determined by the pore space geometry and by phase saturations.

Let us discuss injection of miscible gas which is insoluble in water. Gas-condensate and gas form binary non-wetting oleic phase. The displacing gas is non-wetting and mobile, so it occupies the same domain in the porous space as the displaced gas-condensate. Therefore, the mixing of gas-condensate with gas occurs only inside the active phase. At each moment the ganglia which are separated from the active phase by water are inaccessible for gas injected (Figure 1(b)).

Figure 2 presents variation of active and trapped phases during gas injection into porous media with residual gas-condensate and water after waterflooding. At the beginning of injection gas forms active phase with a small saturation, gas-

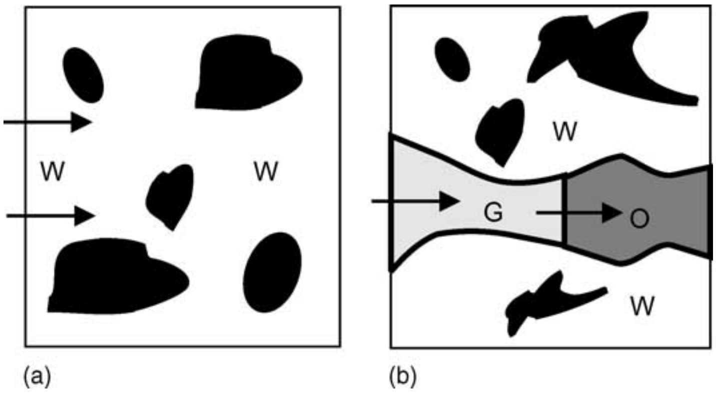

Figure 1. Schematic for the basic statement that miscible gas mixes with active phase only. (a) Trapped oil after waterflood is in state of separated ganglia. (b) During the displacement there are active and trapped phases.

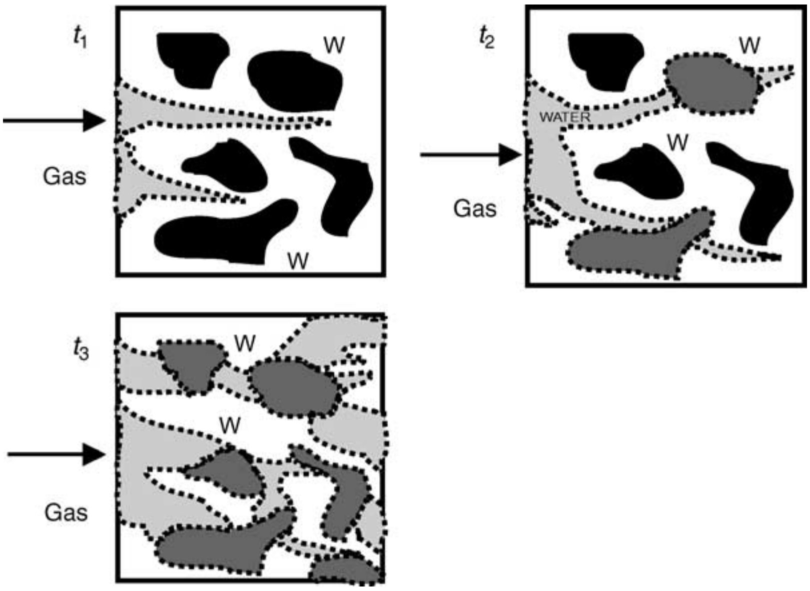

Figure 2. Oil ganglia join the active gas during the injection: development of oleic phase at three different times.

condensate is in state of separated ganglia (moment t_1). During gas injection the saturation of active phase increases, and some ganglia join it (moment t_2). Only at this stage the injected gas reaches ganglia. At the late stage (moment t_3) all the ganglia join the active phase.

So we introduce saturation of the overall oleic phase and saturations of the active and of the trapped oleic phases

$$s = s_\mathrm{a} + s_\mathrm{t} \tag{1}$$

The oleic phase consists of gas and gas-condensate components.

Propagation of injected gas is going on inside the connected mobile phase, so this gas is dissolved in the active phase only (Figure 1(b)). Due to insolubility of gas in water, gas-condensate ganglia are inaccessible for gas until the ganglia join the active phase during the increase of the active oleic phase saturation with gas injection. During drainage and imbibition processes with the variation of oleic phase saturation ganglia join and disjoin the active oleic phase, so there is mass transfer between the active phase and the trapped phase.

2.1. WATER BLOCKING FUNCTION

Let us recall some basic statements on the two-phase displacement of immiscible phases in porous media.

The residual gas-condensate after the waterflooding forms a set of separated ganglia in water-wet porous media (Figure 1(a)). The mechanism of gas-condensate

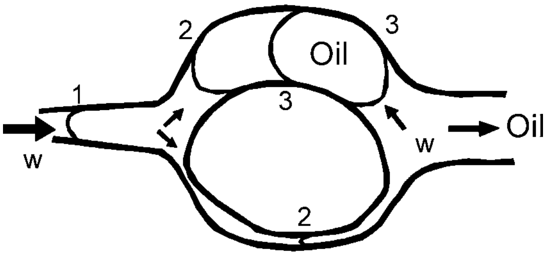

Figure 3. Formation of trapped oil droplet after waterflooding; 1,2,3-positions of the oil–water menisci at three different moments.

trapping in porous media is shown in Figure 3 for the case of the displacement of gas-condensate by water in two capillaries of different radii. At the first moment the meniscus enters in the loop. The meniscus in the thin capillary propagates faster than in the thick capillary (moment 2) because at the low flow velocities capillary force dominates the viscous force. After passing the outlet capillary junction, the meniscus from the thin pore imbibes into the thick pore and traps the gas-condensate drop (moment 3).

After the trapping the flow of water continues in the thin pore. Water in the thick pore is immobile due to the gas-condensate plug. Therefore, the pressure drop on the gas-condensate droplet equals the difference of the pressure in water phase between two junction points. This pressure drop deforms menisci of the trapped drop (Figure 4). The downstream meniscus has a lower curvature than the upstream meniscus. Therefore, the upstream capillary pressure is higher than the downstream capillary pressure, and the resulting capillary force equilibrates the 'outer' pressure drop across the gas-condensate droplet. For thin capillaries and low pressure gradients, which are typical for porous media and gas-condensate–water flows, the pressure drop across a single separated droplet will always be

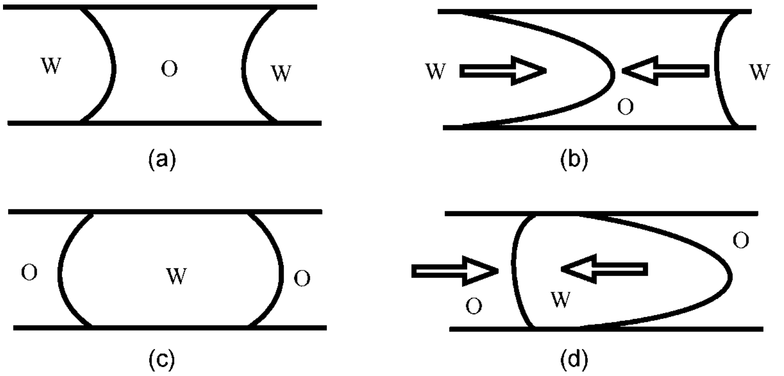

Figure 4. Immobility of oil and water droplets in capillary. Application of the pressure gradient causes deformation of the droplet, and the resulting capillary force equilibrates the outer pressure gradient. (a), (c) – droplets before being submitted to the pressure gradient, (b), (d) – deformed droplets; (a), (b) – oil-wet capillary, (c), (d) – water-wet capillary.

equilibrated by the capillary force. Therefore, separated gas-condensate droplets in water-wet porous media are immobile (see monographs Barenblatt *et al.*, 1987; Dullien, 1992).

The same conclusion relates to the gas-condensate ganglia which occupy the sets of pores. A phase is mobile on the pore scale if and only if it occupies a connected set of pores. The phenomenon of immobility of separated ganglia in porous media is called the Jamin effect.

It takes place for low flow velocity and high interfacial tension, when the capillary number $U\mu/\sigma$ does not exceed 10^{-4}, which is usually the case for conventional fluids in petroleum reservoirs. Here capillary forces strongly dominate over the viscous ones.

So, after the waterflooding gas-condensate is in state of immobile separated ganglia; therefore, during the waterflooding the gas-condensate phase is in two states (Figure 1(b)). The active (continuous) part occupies an 'infinite' cluster of connected pores. Separate ganglia of trapped gas-condensate occupy finite clusters.

Under capillary dominant conditions the picture of the filling of thin and thick pores by wetting and non-wetting phases is determined by capillary forces, that is, by the geometry of the pore network and by the pore radii. Wetting phase tends to fill thin pores and high curvature areas, non-wetting phase moves into thick pores. Therefore, for each moment of displacement the placing of wetting and non-wetting phases in porous space is determined by saturation. This is the reason why relative permeabilities and capillary pressure are functions of saturation only. By the same reason the active gas-condensate saturation is a function of the total gas-condensate saturation:

$$s_{\mathrm{a}} = s_{\mathrm{a}}(s) \tag{2}$$

The function (2) introduced depends on the pore space geometry and is independent of flow velocity, interfacial tension and phase viscosities.

The scenarium for development of active and trapped phases during the displacement (Figure 2) allows to formulate the properties of active saturation function (Figure 5):

- if gas-condensate saturation is lower than the threshold saturation s_{or}, gas-condensate forms finite clusters only, and s_{a} is zero;
- the larger the gas-condensate saturation the lower the trapped gas-condensate saturation (Figure 6), so the function $s - s_{\mathrm{a}}(s)$ decreases monotonically, and the function $s_{\mathrm{a}}(s)$ increases monotonically;
- only a part of the overall gas-condensate saturation belongs to the active continuous gas-condensate, so s_{a} is lower than s;
- at some large value of the saturation s_{g} a connected cluster joins all ganglia, and s_{a} coincides with s.

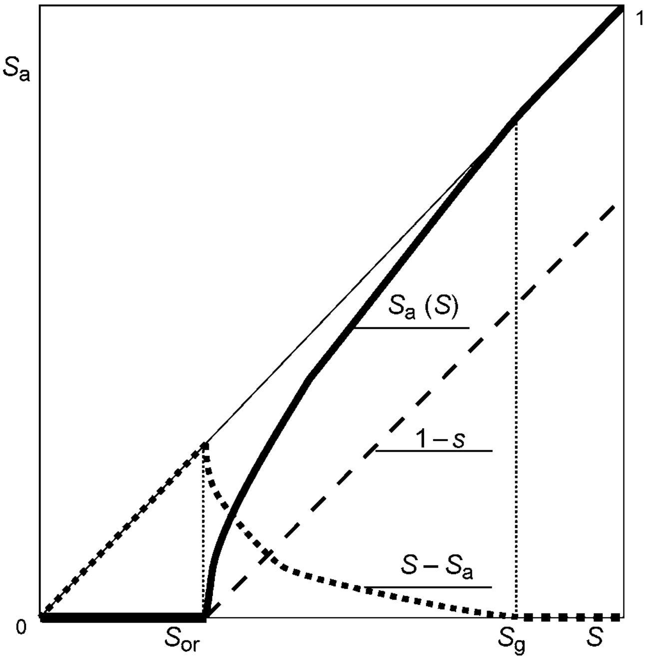

Figure 5. Shapes for active saturation function (continuous line) and for trapped saturation function (dotted line).

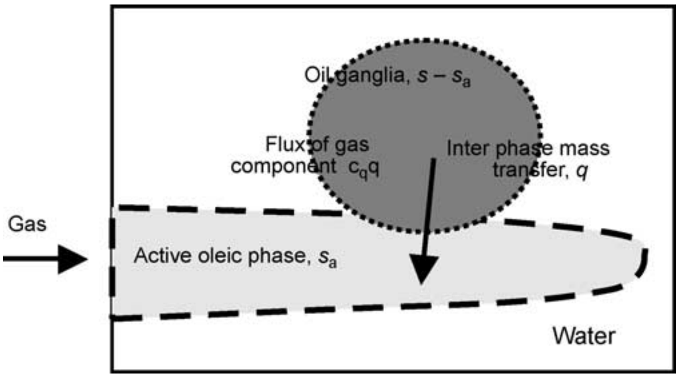

Figure 6. Interphase mass transfer between active oleic phase and trapped ganglia.

A rough estimate of the shape of function $s_a(s)$ can be given by a simplified percolation model. It is assumed in monographs (Stauffer and Aharony, 1992; Seljakov and Kadet, 1997) that pore network is a regular grid with stochastically distributed pore radii (Figure 7). It is assumed also that the wetting phase fills thin pores and non-wetting phase fills thick pores, which is a simplified description but gives realistic shapes for relative permeability curves. Active non-wetting phase fills infinite cluster of thick pores and ganglia of non-wetting phase fill finite clusters.

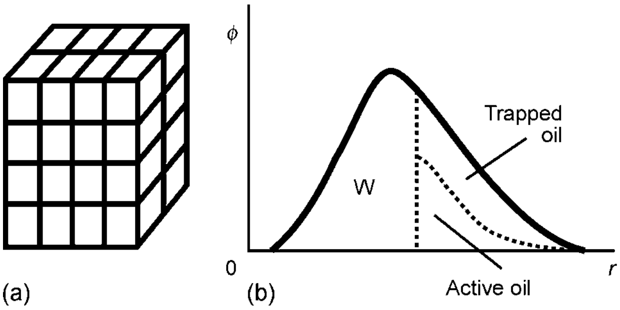

Figure 7. Percolation model for two-phase flow with ganglia: (a) periodical grid of capillary (b) probabilistic distribution of capillary radii.

The formula for density of infinite cluster allows to calculate functions $s_{\mathrm{a}}(s)$ and $s - s_{\mathrm{a}}(s)$. The shapes of functions obtained by the percolation model are the same as the ones in Figure 5.

2.2. LABORATORY MEASUREMENTS OF ACTIVE SATURATION FUNCTION

The active phase saturation function was determined from the experimental data obtained in a paper by Raimondi and Torcaso (1964).

Cores were saturated by gas-condensate and water at fixed saturation. This was done by flooding the core with gas-condensate and water at the desired gas-condensate–water ratio until steady-state, that is, q_{o}/q_w the same on the inlet and on the outlet of the core. Then, without any interruption and without change in flow rate, the displacement was started by switching from gas-condensate to solvent injection. The gas-condensate and the solvent were chosen to have equal viscosity and density, so the water distribution over the pore space was not disturbed after the beginning of solvent injection. This was controlled by measurement of the fractional flow of water in the effluent. This fraction remains constant during the displacement, which indicated that steady-state conditions were preserved during the displacement.

Prior to each run the cores were cleaned with alcohol, then flooded with water. Cores were then flooded with gas-condensate at high rate until water vanished in the effluent.

The saturation of the overall gas-condensate phase at various stages was obtained by making an accurate material balance for each of the steps. The amount of trapped gas-condensate for each saturation was calculated as the difference between the initial overall gas-condensate saturation and the amount of gas-condensate displaced up to the moment when gas-condensate disappears in the effluent. It allowed to calculate the desired dependence $s_{\mathrm{a}}(s)$ (Figure 8).

Three types of porous media were used: consolidated Berea sandstone, crushed Berea sandstone and artificially consolidated Silica sandstone. One curve for Berea

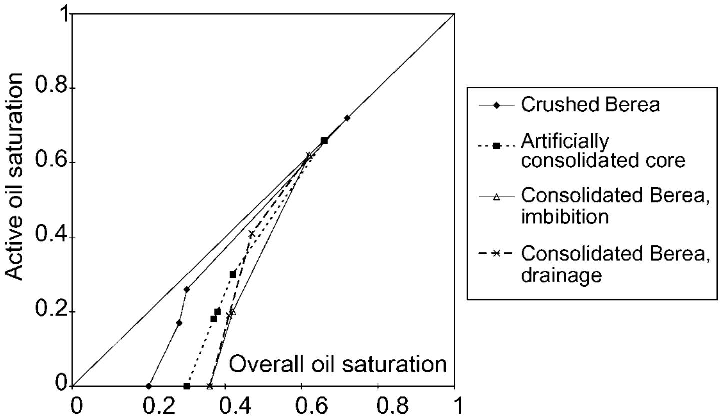

Figure 8. Active saturation function obtained by direct laboratory measurements for three different cores.

sandstone was obtained by imbibition, another curve for Berea sandstone was obtained by drainage.

The shapes of four curves 1–4 shown in Figure 8 fulfil the above formulated features of the active saturation function, which have been formulated from intuitive speculations.

2.3. WATER BLOCKING FUNCTION FROM HYSTERETIC RELATIVE PERMEABILITY

Let us discuss primary drainage and imbibition in a water-wet core.

With the primary drainage, gas-condensate occupies an infinite cluster of the connected network of the thick pores only. There is no gas-condensate in the core before the primary drainage and no mechanism which can separate gas-condensate from its active part (Figure 9(a)). Primary drainage results in separation of some water droplets which are left in porous media after the process, and in creation of the water film which fills areas of a high curvature (Figure 9(b)). Further with the imbibition process the active gas-condensate phase shrinks due to increasing water saturation and also due to separation of gas-condensate ganglia (Figure 9(c)). This is the conventional explanation of relative permeability and capillary pressure hysteresis (see monographs Aziz and Settari, 1979; Lake, 1989).

Let us assume that relative permeability for gas-condensate is dependent of the saturation of the accessible gas-condensate only and is independent of the saturation of discontinuous immobile gas-condensate. This allows to calculate the function $s_a(s)$ from gas-condensate relative permeability curves for the primary drainage and imbibition (curves 1D and I in Figure 10).

For any arbitrary value k_{ro} the value of the argument on the gas-condensate relative permeability curve I is s, which is the sum of saturations for the active and inaccessible gas-condensate. Relative permeability k_{ro} is function of s_a only.

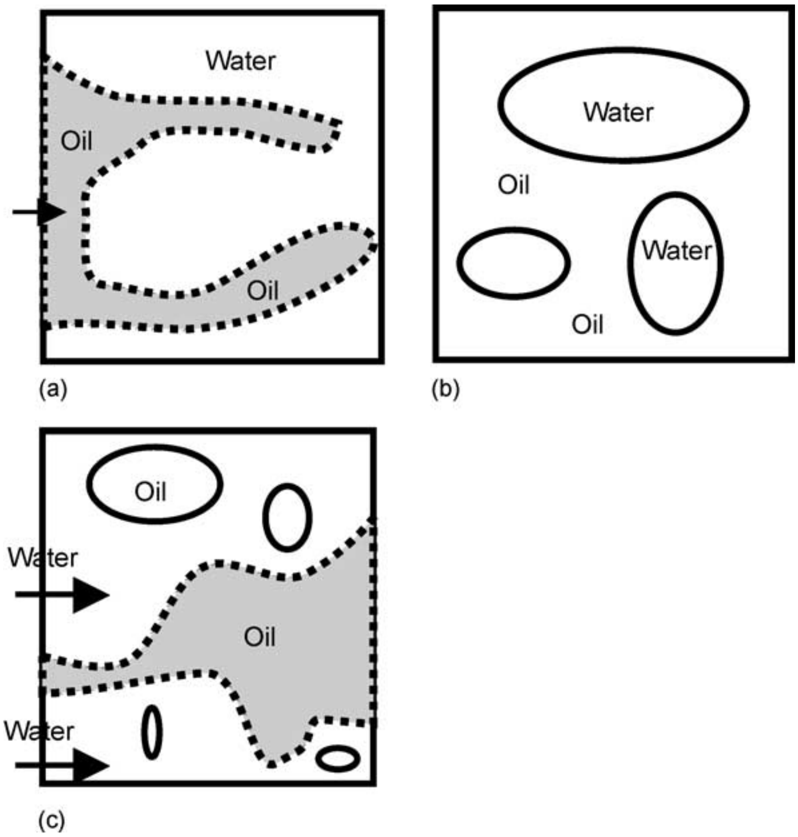

Figure 9. Hysteresis of oil relative permeability due to oil ganglia.

During the primary drainage s_{a} coincides with s, thus, the argument value on the curve 1D is equal to s_{a}. So we end up with the relationship:

$$k_{\mathrm{ro}}^{\mathrm{1D}}(s_{\mathrm{a}}) = k_{\mathrm{ro}}^{\mathrm{I}}(s) \tag{3}$$

It allows to calculate the function $s_{\mathrm{a}}(s)$ as an inverse function from (3) (Figure 10).

For the shape of relative permeability curves, shown in Figure 10, the properties of the active saturation function $s_{\mathrm{a}}(s)$, which have been formulated in one of previous sections, are fulfilled, the shape of the function is the same as the one given in Figure 5. Relative permeability for the primary drainage 1D and imbibition I differ from each other up to the point of interstitial water saturation, so gas-condensate ganglia do exist even at high gas-condensate saturation below s^0. Therefore, the point s^0 for the case of curves in Figure 10 coincides with the point g where all ganglia join the continuous cluster (see Figure 5).

The proposed method can be verified using relative permeability curves for the first drainage and for the imbibition obtained experimentally in the mentioned above work (Raimondi and Torcaso, 1964). Active saturation function for two cores

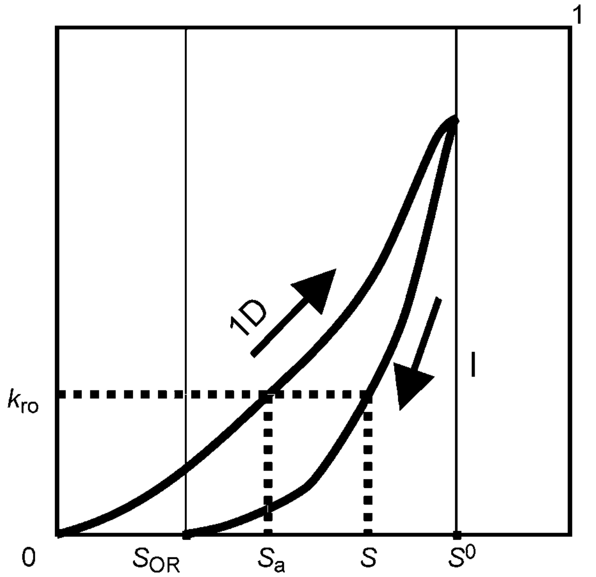

Figure 10. Relative permeability for oil is higher for primary drainage then for imbibition.

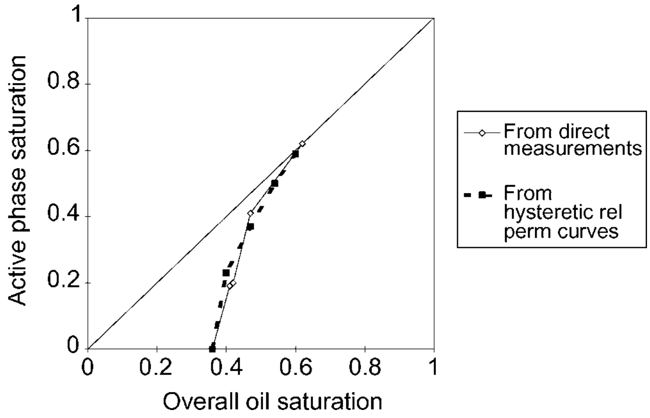

Figure 11. Active saturation function obtained from hysteretic relative permeability curves and from direct measurements, Berea sandstone.

have been calculated above based on direct measurements presented in the same work (Cullick *et al.*, 1993) (Figures 8, 11 and 12). The dotted curve in Figure 11 was obtained by the formula (3) from hysteretic relative permeability curves for the Berea sandstone, the continuous curve is a plot of the active saturation function obtained from the steady state displacement data from the same core (the points are taken from Figure 8).

One can observe a fairly good agreement between the two curves obtained by two different methods.

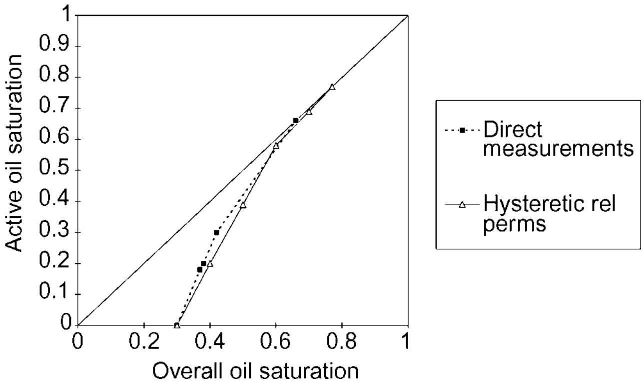

Figure 12. Comparison of active saturation obtained from hysteretic relative permeability curves and from direct measurements, artifially consolidated Silica sand.

Figure 12 presents the same data for the artificially consolidated Silica sand. The continuous curve was obtained from hysteretic relative permeabilities using formula (3). The dotted curve was obtained from the displacement data (the points are taken from Figure 8).

For both cores, relative permeability for gas-condensate for the processes 1D and I coincide at high values of saturation below s^0, therefore the point g is located to the left of the point of maximum saturation s^0.

So, the laboratory measurements give the same shape of the active saturation function as the one which has been predicted from the qualitative analysis of the growth of ganglia population, and also as the shape of the active saturation function given by the percolation model. Besides, very good quantitative agreement between values of the active saturation function obtained from the laboratory mass balance measurements and from hysteretic relative permeability was observed. So, the hypothesis that the active phase saturation is a function of the overall phase saturation has been verified experimentally.

2.4. MASS EXCHANGE BETWEEN ACTIVE PHASE AND GANGLIA

Let us determine terms of inter phase mass transfer between active and trapped phases by the gas component q_{c}^{m} and by the gas-condensate component $q_{1-\mathrm{c}}^{m}$ (Figure 6). The scenario of joining ganglia to the increasing oleic phase (during miscible gas injection into the porous medium with water and residual gas-condensate) is shown in Figure 2 for three different moments. There were some separated immobile gas-condensate ganglia in porous media after water injection. During injection of gas, the saturation of active oleic phase increases (Figure 2, moment t_1) due to supply of gas and due to ganglia joining the active phase. With the joining of some ganglia to the active phase, saturation of the trapped phase decreases (moment t_2). At high oleic phase saturation, all ganglia join active phase and the trapped phase disappears (moment t_3).

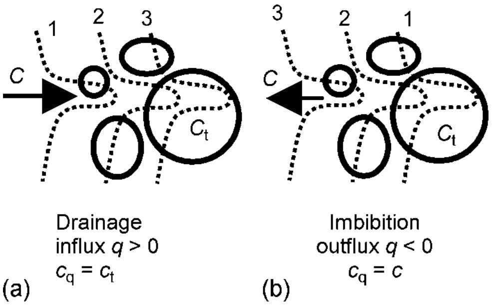

(a) Drainage
influx $q > 0$
$c_q = c_t$

(b) Imbibition
outflux $q < 0$
$c_q = c$

Figure 13. Mass exchange between active phase and ganglia.

The volume of oleic phase which moves from the trapped phase to the active phase per unit of time in the unity volume of porous media q equals to time derivative of ganglia saturation:

$$q = -\frac{\partial s_t}{\partial t} \tag{4}$$

During the drainage process, saturation of overall oleic phase increases, saturation of ganglia decreases, some ganglia join active phase and disjoin the trapped phase. So there is an influx in the active phase, and the joining ganglia transfer oleic phase from the trapped phase, the average gas concentration in transferring flux is c_t^m, see Figure 13(a).

During the imbibition process, the saturation of the overall oleic phase decreases and the saturation of ganglia increases, some ganglia disjoin active phase and join the trapped phase. So, there is an outflux from the active phase. At each moment density and gas concentration of ganglia which leave the active phase equals the average density and gas concentration c^m inside the active phase, see formula (A.5) (Figure 13(b)).

2.5. 1-D DISPLACEMENT WITH CONSERVED FLUX

Amagat's law means that the volume of the mixture equals to the sum of volumes for individual components. It allows the introduction of volume concentrations of each component with the total of concentrations equals to unity (see Lake, 1989; Bedrikovetsky, 1993):

$$\rho_O c^m = \rho^G c; \quad \rho_O(1 - c^m) = \rho^O(1 - c) \tag{5}$$

Here ρ^G and ρ^O are densities of individual components which are assumed to be constant.

Let us derive equations for 1-D displacement of 2-phase 3-component Amagat's fluids.

Substituting the Amagat law (5) in Equations (A.2) and (A.3), cancelling the constant individual densities and adding these two equations to the water balance equation (A.1) we obtain the conservation of the total flux: $U = U(t)$.

Introducing dimensionless linear coordinate and time

$$X = \frac{x}{L}; \qquad T = \frac{\int_0^t U^0(\tau)d\tau}{\phi L}; \qquad u = \frac{U}{U^0(t)} \tag{6}$$

we obtain volume balance for the overall oleic phase:

$$\frac{\partial s}{\partial T} + \frac{\partial f(s, c)}{\partial X} = 0 \tag{7}$$

The volume balance equation (A.2) for gas component in both oleic phases in dimensionless coordinates becomes:

$$\frac{\partial[cs_{\mathrm{a}} + c_{\mathrm{t}}(s - s_{\mathrm{a}})]}{\partial T} + \frac{\partial cf}{\partial X} = 0 \tag{8}$$

Equation (A.7) takes the form:

$$\begin{aligned} &\frac{\partial c_{\mathrm{t}} s_{\mathrm{t}}}{\partial T} = c_{\mathrm{t}} \frac{\partial s_{\mathrm{t}}}{\partial T}, \quad \frac{\partial s}{\partial T} < 0 \\ &\frac{\partial c_{\mathrm{t}} s_{\mathrm{t}}}{\partial T} = c \frac{\partial s_{\mathrm{t}}}{\partial T}, \quad \frac{\partial s}{\partial T} > 0 \end{aligned} \tag{9}$$

The system of three equations (7)–(9) is closed. It determines three unknowns: $s(X, T)$, $c(X, T)$ and $c_{\mathrm{t}}(X, T)$.

For drainage processes and for imbibition processes system (7)–(9) can be reduced to two equations.

Differentiation by parts of the left hand side of the first equality (9) results in the following conclusion for drainage:

$$\frac{\partial c_{\mathrm{t}}}{\partial T} = 0, \quad c_{\mathrm{t}} = c_{\mathrm{t}}(X) \tag{10}$$

During the drainage process ganglia join the active phase, and concentration of gas in the remained ganglia remains the same. So, considering initial distribution of gas in gas-condensate ganglia $c_{\mathrm{t}}(x, t = 0)$, there is no way to change it during drainage.

The model for displacement consists of Equations (7) and (8), where concentration in ganglia $c_{\mathrm{t}}(X) = c_{\mathrm{t}}(X, T = 0)$ is a known function.

For imbibition process, the substitution of expressions for the mass exchange (9) into the mass balance (7) and (8) results in the equation:

$$\frac{\partial c}{\partial T} + \frac{f(s, c)}{s_{\mathrm{a}}} \frac{\partial c}{\partial X} = 0 \tag{11}$$

So variation of gas concentration in active gas-condensate is independent of the gas concentration in ganglia, because during imbibition the saturation of gas-condensate ganglia decreases, ganglia disjoin from the active gas-condensate phase, influx into ganglia phase changes gas concentration in ganglia, but the content of gas in the active phase is not affected (Figure 13).

The variation of gas concentration in ganglia c_t is determined after the solution of the system (7) and (11) from the first equation (9):

$$c_t(x,t) = \frac{1}{s - s_a(s)} \left(c_t(x,0)(s_i - s_a(s_i)) + \int_0^t c \frac{\partial (s - s_a(s))}{\partial \tau} d\tau \right) \tag{12}$$

The imbibition process is described by the system of two equations (7) and (11) with unknowns $s(X,T)$ and $c(X,T)$, concentration $c_t(X,T)$ is found from the expression (12).

3. Analytical Model for 1-D Flows

Let us discuss displacement of gas-condensate and water by the miscible gas with water:

$$T = 0{:}\quad s = s_I;\ c = 0;\ c_t = 0; \qquad X = 0{:}\quad f = f^0;\ c = 1 \tag{13}$$

The solutions are self-similar and are dependent on one coordinate X/T only:

$$s(X,T) = s(\xi); \qquad c(X,T) = c(\xi); \quad \xi = X/T \tag{14}$$

The fraction f^0 of gas in the injected water–gas fluid can be expressed via the ratio of water and gas fluxes (so called WAG-ratio): $f^0 = 1/(1 + \text{WAG})$.

We denote values of the initial state as I, and values of the injected state as J. The solution of the problem (13) corresponds to a path on the plane (s, c) which links points (s_J, c^0) and $(s_I, 0)$.

For the sake of simplicity we discuss the simplified case where fractional flow function is independent on concentration, which corresponds to equality of gas-condensate and gas viscosities. In this case the Equation (7) can be separated from Equations (8) and (9), and these equations become linear.

Analytical solutions with varying fractional flows help to understand how much gas-condensate is left in porous media after the injection of water with miscible gas. Let us try to guess the answer in advance.

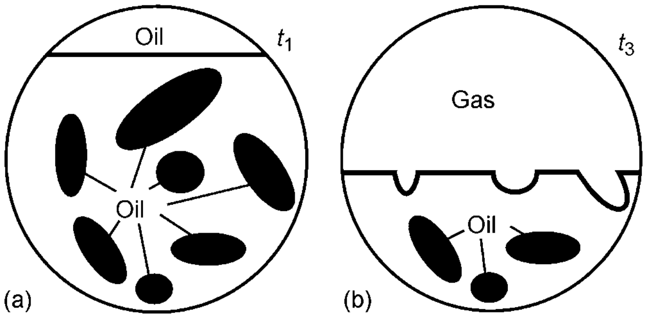

Figure 14. Schematic for consuming the oil ganglia by active oleic phase during drainage.

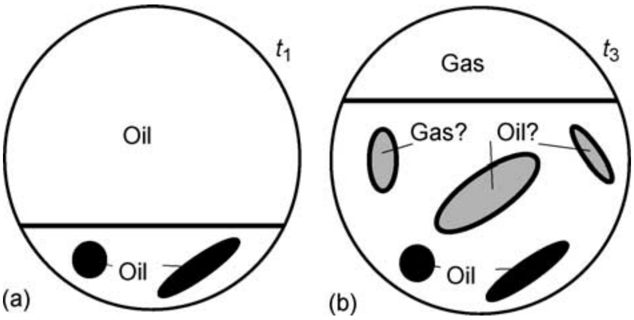

Figure 15. Schematic for appearance of gas ganglia during imbibition.

Initially porous medium is saturated by gas-condensate and water, and some gas-condensate ganglia are trapped by water (Figure 14(a) and Figure 15(a)).

If the fractional flow of gas in the injected mixture is higher than the fractional flow for gas-condensate in the displaced gas-condensate–water fluid, the drainage process takes place, and oleic phase saturation increases. Some gas-condensate ganglia join the active phase where the mixing of the displaced gas-condensate with the injected gas happen (Figure 14(b)) shows the schematic for phases after the displacement). No mixing happen in ganglia. So, saturations of active phase and of ganglia after the displacement are determined by the fractional flow of injected gas–water mixture and are independent of initial saturations, concentration of gas-condensate in the active phase equals zero and concentration of gas-condensate in the residual ganglia equals unity (Figure 14(b)).

The ganglia which consist of the pure gas-condensate, are called 'black' ganglia.

If the fractional flow of gas in the injected mixture is lower than the fractional flow for gas-condensate in the displaced gas-condensate–water fluid, the imbibition process takes place, and oleic phase saturation decreases (Figure 15(b)) shows active and trapped oleic phases after the displacement). Some ganglia disjoin the active oleic phase. The question is whether these ganglia consist of gas-condensate, gas or gas–gas-condensate mixture (i.e. the disjoining ganglia are black, white or grey, correspondingly). The answer depends on velocities of oleic and water phases.

If oleic phase moves faster than water, at first gas displaces gas-condensate inside the active phase in each point of the porous medium, and then ganglia disjoin active phase when the saturation front arrives. In this case disjoining ganglia consist of gas only (i.e. they are white).

If water moves faster than the oleic phase, saturation front reaches each point of the reservoir faster than the concentration front. So disjoining ganglia consist of gas–condensate only.

One could expect the intermediate cases where disjoining ganglia consist of the gas-condensate–gas mixture (i.e. they are grey).

So, after the displacement by imbibition, saturations of active and trapped phases are also dependent of gas–water ratio of the injected fluid but are at the same time dependent of initial saturations. There is also no gas-condensate left in the active phase after the displacement. The ganglia which have been in reservoir before the displacement consist of gas-condensate only. The ganglia which disjoin from active phase during imbibition could consist of gas, of gas-condensate and of gas-condensate–gas mixture, depending on which phase velocity is higher.

Let us see whether the analytical solutions confirm the initial guess.

3.1. COMPARISON WITH LABORATORY TESTS

Let us discuss first the simple case of injection of water–solvent mixture with a fraction of water which equals the water fraction in the initial water–gas-condensate mixture in the reservoir: $f^0 = f(s_\mathrm{I})$.

The solution has a piston-like type: $c = 1$ behind the concentration front, and $c = 0$ ahead of the front. The velocity of the displacement front is $V_\mathrm{c} = f^0/s_\mathrm{a}(s_\mathrm{I})$.

Distribution of oleic phase over the porous space remains the same, and position of the horizontal line which separates active oleic phase from water in Figure 14 remains the same. Miscible displacement takes place inside the active phase, which is in accordance with the initially proposed schematic of the process (Figure 1(b)). Gas completely displaces gas-condensate from the active part, gas-condensate remains in ganglia.

The traditional model where $s_\mathrm{a}(s) = s$ also gives a piston-like displacement solution with the constant saturation (Lake, 1989; Bedrikovetsky, 1993). The velocity of the displacement front in this case is $V_\mathrm{s} = f^0/s_\mathrm{I}$.

If compared with the traditional model, the solution obtained exhibits higher velocity of the piston like front, $V_\mathrm{c} = f^0/s_\mathrm{a}(s_\mathrm{I}) > f^0/s_\mathrm{I}$. It corresponds to the fact that the injected solvent propagates inside the active phase through the 'cross section with the area $s_\mathrm{a}(s_\mathrm{I})$', while the traditional model assumes the cross-section area equals to the overall gas-condensate saturation s. From the point of view of the recovery, according to the model proposed, gas-condensate ganglia are left behind the piston like front, so it takes less time to produce all the gas-condensate when compared with the case of the total displacement with the same gas-condensate–water ratio at the outlet. The amount of gas-condensate trapped is $s_\mathrm{I} - s_\mathrm{a}(s_\mathrm{I}) = f^0(1/V)_\mathrm{s} - 1/V)$.

The solution obtained has been compared with results of laboratory displacement in Raimondi and Torcaso (1964) work. The tests are the same as the ones given in Figures 8, 11 and 12. Here we discuss two runs (No. 2 and No. 4) where continuous injection of the gas-condensate–water fluid was switched to injection of the solvent–water fluid, ratios water/gas-condensate and water/solvent were the same, and gas-condensate and solvent have the same viscosity and density.

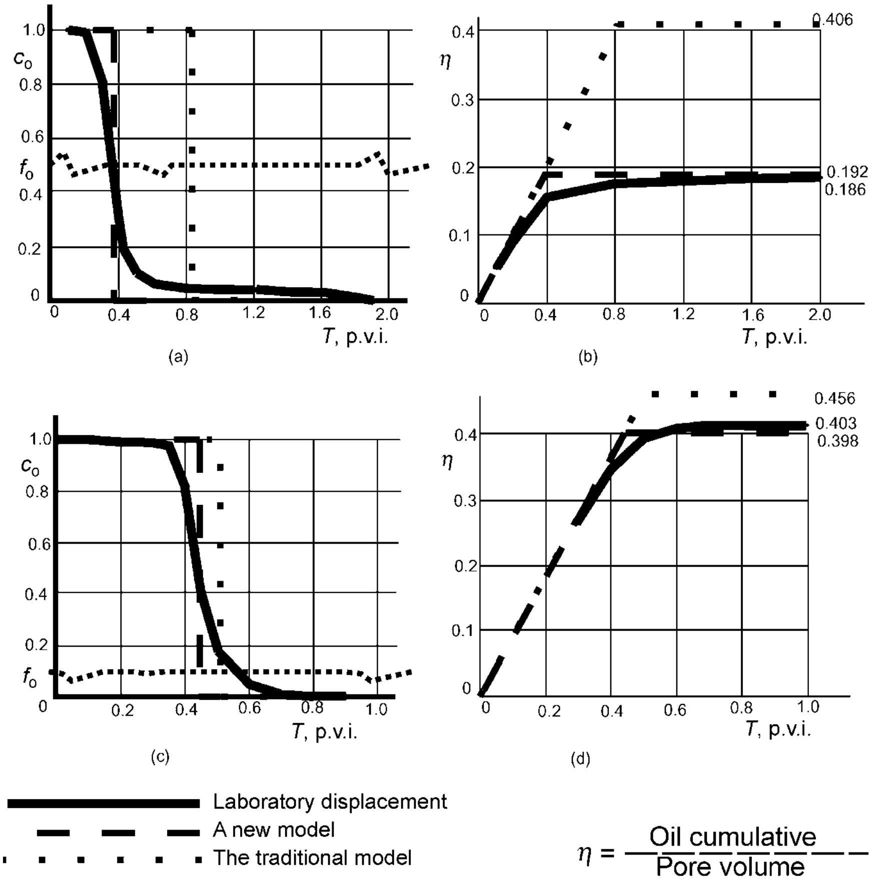

Figure 16. Comparison of laboratory data with results of analytical modelling: (a) concentration at the outlet, run 2; (b) recovery factor, run 2; (c) concentration at the outlet, run 4; (d) recovery factor, run 4.

It was observed during the laboratory test that the water cut at the outlet was almost constant, $f(X = 1, T) = f^0 = f(s_I)$ (Figure 16(a) and (c)), the same as in the obtained solution.

The measured concentration in the core outlet and the cumulative recovery during the displacement from Berea sandstone are given in Figure 16(a) and (b) for gas-condensate–water ratio 0.96 and in Figure 16(c) and (d) for gas-condensate–water ratio 9,94. The core is relatively short (72 in) for the piston-like profile to be expected. Diffusion and non-equilibrium of dissolution of gas-condensate in solvent smooth the profile. So one could expect better match between the laboratory data and the results of modelling in large scale approximation for final recovery rather than for the dynamics of concentration.

For both tests experimental data are matched by the 'ganglia model' much better than by the traditional model.

For the first case (Figure 16(a) and (b)), position of the piston-like concentration front given by the obtained analytical solution with concentration front velocity $V_c = f^0/s_a(s_I)$ almost coincides with the 'centre of mass' for the profile with laboratory displacement. The velocity of the front given by the traditional model is much lower. The arrival time predicted by the ganglia model is 0.39 p.v.i. while the traditional model gives the value 0.83 p.v.i. (Figure 16(a)). Such a large difference in arrival times corresponds to the large difference between active saturation $s_a(s_i) = 0.192$ and overall saturation of oleic phase $s_i = 0.406$. The cumulative recovery curve (Figure 16(b)) shows that the final recovery (0.186) almost coincides with the amount of gas-condensate in the 'active' mobile state (0.192), and ganglia are not recoverable.

For the second case (Figure 16(c) and (d)) also a good agreement between the laboratory data and the modelling results was observed. Difference between active phase saturation (0.398) and overall oleic phase saturation (0.456) is lower than in the first case. Therefore, difference in arrival times given by solution obtained (0.44 p.v.i.) and by the traditional model (0.51 p.v.i.) is lower also. The final recovery is 0.403 (Figure 16(d)) which almost coincides with the active gas-condensate saturation, 0.398.

So the introduction of active and trapped phases in mathematical model results in a significant improvement of the matching of the experimental data by the modelling results.

3.2. WAG WITH DRAINAGE

Now let us discuss WAG with drainage, where WAG-ratio is lower then the initial water–gas-condensate ratio in the reservoir, $f^0 > f(s_I)$.

The equation for saturation is (7), concentration can be found from Equation (8). Initial concentration of gas in ganglia equals zero, so it remains zero during the displacement (10).

The solution for the 'separate saturation-problem' (7) is given by a full shock J → I, the velocity V_s of the front is determined by the Hugoniot condition of the water balance on the shock front.

Let us discuss the Hugoniot condition of material balance for gas component on the concentration shock. As it follows from conservation law (8), the velocity of the concentration shock is

$$V_c = \frac{c^- f^- - c^+ f^+}{c^- s_a^- - c^+ s_a^+} \tag{15}$$

For the region on the plane (X, T) outside the saturation jump where $s = \text{const}$ equation (8) degenerates into the linear hyperbolic equation (11) with constant characteristic velocity.

The velocity of concentration shock for Equation (11) is: $V_c = f/s_a$. The same expression follows from the Hugoniot condition (15) for $c^- = 0$ or $c^+ = 0$.

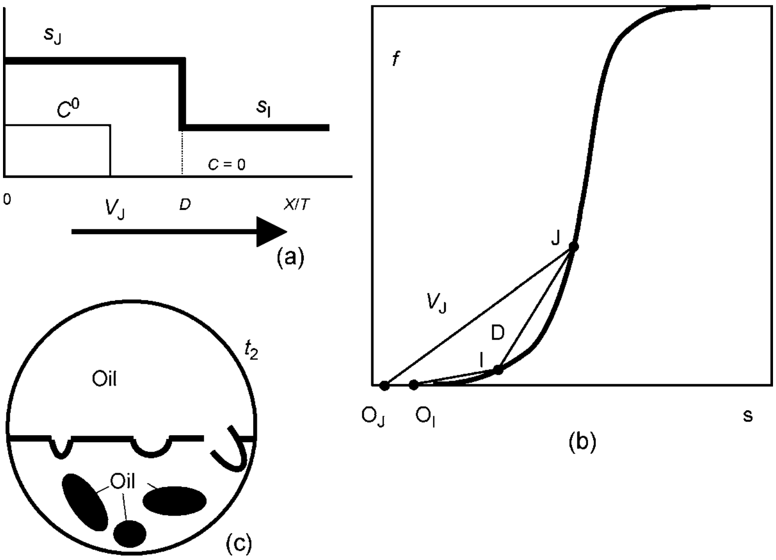

Figure 17. Saturation and concentration profiles for miscible WAG with drainage.

The velocity V_c can be calculated geometrically on the plane (s, f) (Figure 17). Let us mark the point O with coordinates $(s - s_a, 0)$. The tangent of the slope of the straight line O–(s, f) equals V_c.

For points I and J shown in Figure 17(b) we have $V_s > V_J > V_I$. So, the concentration shock cannot coincide with the saturation shock. Therefore, the trajectory of concentration front lies either ahead of the saturation front, or behind it. But the velocity of the saturation front is higher than the velocity of the concentration front. So, the concentration front lags behind the saturation front.

See saturation and concentration profiles in Figure 17(a).

This solution allows to calculate the amount of residual (remaining) gas-condensate after miscible WAG injection under drainage conditions. Initially there was $s_a(s_I)$ of the active gas-condensate and $s_I - s_a(s_I)$ of ganglia in porous media (cross-section of the core is shown in Figure 14(a)).

If during WAG injection the drainage happens, saturation of the active oleic phase increases and ganglia join it. So, there is no chance for gas to get into ganglia, and remaining ganglia consist on gas-condensate component only. The amount of residual gas-condensate equals the trapped phase saturation. After the displacement there is $s_a(s_J)$ of gas and $s_J - s_a(s_J)$ of gas-condensate in porous media (cross-section of the core is shown in Figure 14(b)). The amount of residual gas-condensate and the recovery factor after WAG are:

$$s_{or}(f^0) = s_a(s_J), \qquad f^0 = f(s_J), \qquad \eta = \frac{s_I - s_a(s_J)}{s_I} \tag{16}$$

The graphical procedure for calculation of the residual gas-condensate after miscible WAG is shown in Figure 18. The simplified assumption of the

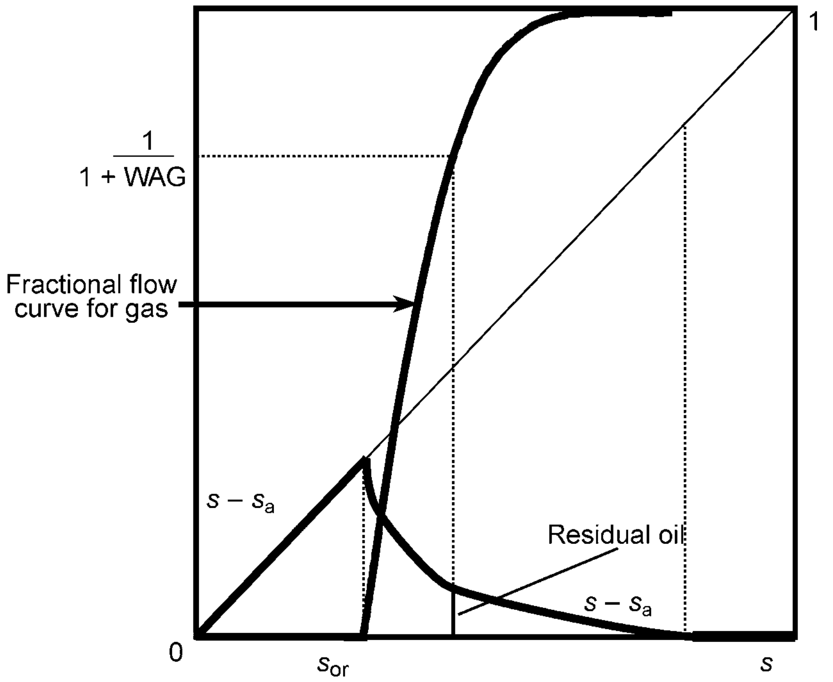

Figure 18. Incremental recovery for tertiary WAG with drainage.

independence of fractional flow function on concentration results in the single fractional flow curve involved with the solution (Figure 17). When one calculates the residual gas-condensate, the active part of oleic phase is filled by gas, so the fractional flow curve for system water–gas is to be considered. The saturation s_J is determined from the fractional flow curve 'water–gas'. Saturation of the trapped gas-condensate $s_J - s_a(s_J)$ is determined from the plot of the trapped gas-condensate versus overall saturation (Figure 18).

Fractional flow for gas is very high even for low saturation due to the low gas viscosity (Figure 18). Therefore, even for high value of f^0 (for low water–gas ratio), saturation s_J is lower than s_g, so, some ganglia remains unswept by the miscible WAG.

The plot of the residual gas-condensate versus fractional flow of injected gas is shown in Figure 19. The part of the curve which corresponds to the drainage process lies to the right of the initial reservoir point I. The residual gas-condensate decreases with the increase of f^0. It decreases, from the value s_{or} for the water flooding, slowly for the values of f^0 up to 0.5–0.6. For high values of f^0 the residual gas-condensate decreases faster, and it becomes zero for $f^0 = f(s_g)$.

It is important to emphasise that according to the traditional model for miscible WAG, which does not take into account gas-condensate ganglia, residual gas-condensate saturation after WAG equals to zero for any WAG-ratio from zero to infinity (Lake, 1989; Bedrikovetsky, 1993).

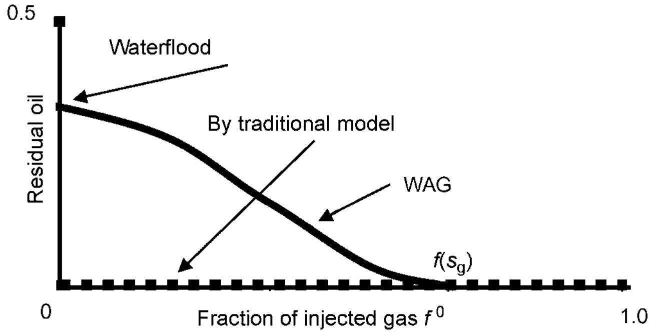

Figure 19. Residual oil after miscible WAG with drainage.

3.3. WAG WITH IMBIBITION

Let us discuss continuous WAG injection with a water–gas ratio (WAG-ratio) higher than the initial water–gas-condensate ratio in the reservoir, $f^0 < f(s_I)$. The injection point J is located on the phase plane below the initial point I (Figures 20–24). The equation for saturation is (7), concentration can be found from Equation (11). Initial and boundary conditions are homogeneous, (13).

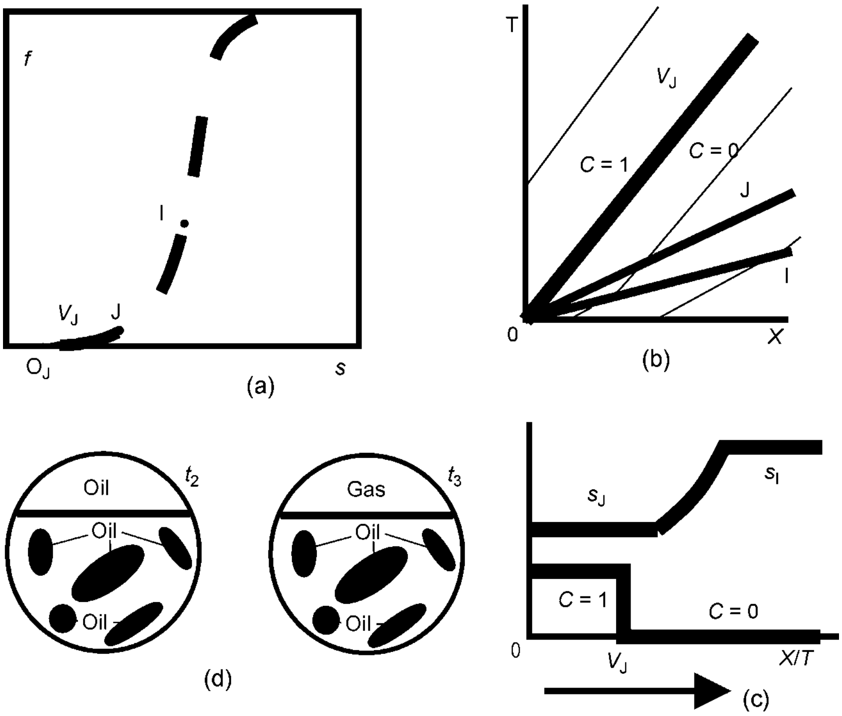

Figure 20. Saturation and concentration profiles for WAG with imbibition and with delayed concentration front.

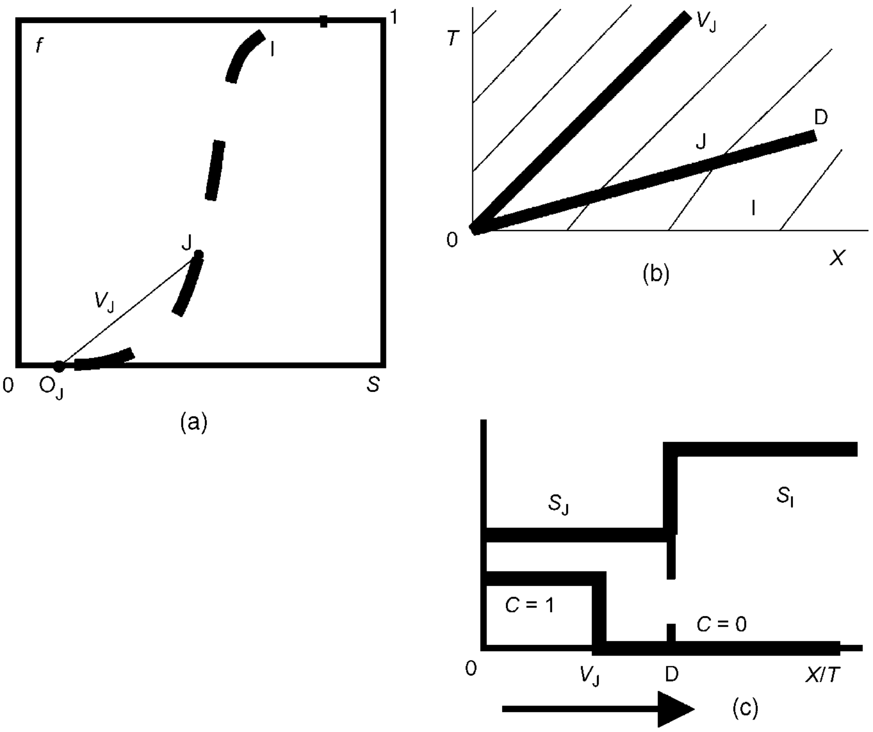

Figure 21. WAG with imbibition and with fast saturation front.

3.3.1. *Black Residual Ganglia*

The relationships between the velocity of the saturation front V_s, velocity of c-characteristic line ahead of the shock V_I and behind the shock V_J depend on the location of points I and J on the (s, f) plane. Let us discuss first the cases of slow concentration front where $V_s > V_c$.

3.3.1.1. *Tertiary WAG with High WAG-Ratio.* If points I and J are located both on the convex part of f–f curve (below the inflection point of f–f curve) (Figure 20(a)), the saturation distribution is given by a rarefaction wave. Here the velocity of the piston-like front of concentration is $V_J = f(s_J)/s_a(s_J)$.

Profiles of saturation and concentration during the displacement are given in Figure 20(c).

Let us calculate the concentration c_t of gas in ganglia. Ahead of the concentration front $c = 0$, so the term under the integral (12) equals to zero. Behind the front the concentration is unity, but saturation does not change, and $q = 0$. Therefore, for the solution presented, the expression under the integral (12) equals zero. The first term in brackets in right hand side of (12) is zero also for the case where there is no gas in initial gas-condensate. Therefore, $c_t(X, T) = 0$.

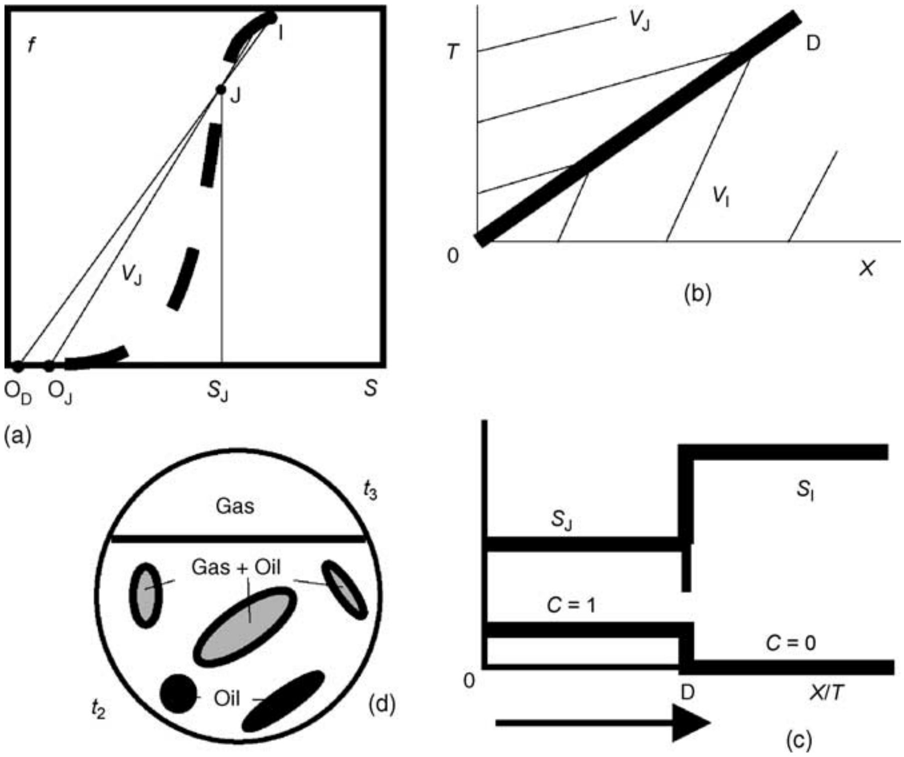

Figure 22. WAG with imbibition and with single saturation-concentration front.

Gas saturation in ganglia behind the saturation front can be found from the Hugoniot condition of the mass conservation for gas on the discontinuity, see (8):

$$(c^+s_a^+ + c_t^+s_t^+ - c^-s_a^- + c_t^-s_t^-)V_c = (c^+f^+ - c^-f^-) \tag{17}$$

Substituting in (17) expression for the velocity of c-characteristic line behind the shock V_J, condition of continuity of saturation on the c-shock $s^- = s^+$, concentrations ahead of the shock $c^- = 0$ and behind the shock $c^+ = 1$, concentration in ganglia ahead of the shock $c_t^+ = 0$, we obtain: $c_t^- = 0$.

Let us interpret the solution obtained. Figure 15(a) presents the initial state in the core before the displacement. The saturation front moves faster than the concentration front (Figure 20(c)). Therefore, these are gas-condensate ganglia which disjoin the active phase after passing the imbibition rarefaction wave of saturation. The schematic for the moment after passing the imbibition wave and before coming the concentration front is shown in Figure 20(d), moment t_2. After passing the concentration front at moment t_3 gas-condensate is displaced by gas from the active phase. So, the ganglia disjoined from the active phase, left after the imbibition, corresponding to grey ganglia in Figure 15(b), are not touched by gas, being, in fact, pure gas-condensate ganglia, black in Figure 20(d).

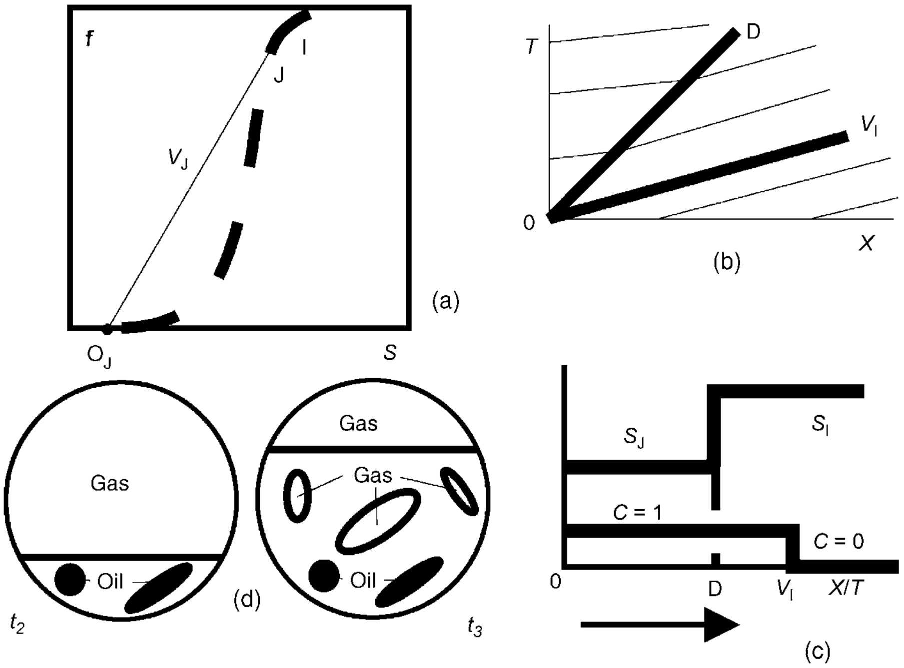

Figure 23. WAG with imbibition and with slow saturation front.

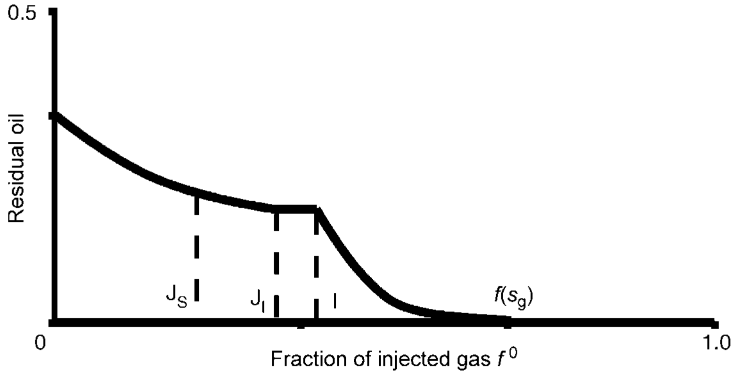

Figure 24. Residual oil after miscible WAG for low initial water saturation.

The important conclusion is that there is no gas left in the trapped gas-condensate after WAG. So the amount of residual gas-condensate equals the saturation of ganglia after WAG which is determined by WAG-ratio applied, formula (16) is valid for this case also.

3.3.1.2. *Medium Initial Saturation and High WAG-Ratio.* Let us determine point J_I which is the tangent point between f–f curve and the interval I–J_I. If initial point I is located above the inflection point of f–f curve, and injection point J is located below the point J_I, the saturation path consists of a sequence of rarefaction wave and shock wave (there will be jump up to the point J after the continuous line in saturation profile, Figure 20(c)).

In this case also velocity of c-characteristic V_c is lower than the velocity of s-wave. The concentration jump lays behind the zone of varying saturation. So all the ganglia left after the displacement consist of gas-condensate only.

3.3.1.3. *Medium Initial Saturation and Medium WAG-Ratio.* Let us determine point 2 in which velocities of c-front and of s-wave coincide: $f/s_a = f/s$, and point J_{II} in which $V_s = V_J$. Another case where $V_s > V_c$ is realised where point I is located below point 2, and point J is located above point J_I (Figure 21). The solution for saturation is given by shock which moves faster than the concentration shock Figure 21(b) and (c). As in the previous case appearance of ganglia on the s-shock is going on under the absence of gas, so there is no gas in ganglia.

Also there is no variation of c_t on the concentration jump, and $c_t^- = 0$. Ganglia which disjoin the active phase after passing the imbibition shock of saturation (Figure 21(d)) consist of gas-condensate only. After the displacement all remaining ganglia are black (Figure 15(b)). In this case the saturation of residual gas-condensate equals the saturation of ganglia after WAG, formula (16).

The same flow regime takes place if point I is located above point 2, and point J is located below J_{II}.

So, for the above described four cases s-velocities in rarefaction and shock waves are higher than c-velocities along the path on the plane (s, f), and all the remaining ganglia consist of gas-condensate only, that is, they are 'black'. The residual gas-condensate is given by formula (16). The plot of residual gas-condensate versus fractional flow of gas–water with WAG injection is shown in Figure 19 (it is the same as for WAG with drainage), the part of the curve which lies to the left of the initial point I corresponds to imbibition processes. If the fractional flow value tends to zero (WAG-ratio tends to unity) the residual gas-condensate tends to the value of the residual gas-condensate after waterflooding.

3.3.2. *Grey Disjoining Ganglia*

Now let us discuss the cases where the s-shock propagates slowly or with the same velocity as the c-shock. It takes place if point I is located above the point 2, and point J is located above the point J_{II}.

Let us mark the point O_I with co-ordinates $(s_{tI}, 0)$ on the plane (s, f) (Figure 22(a)). The slope of the line O_I–I equals to V_I. The intersection points between the line O_I–I and fractional flow curve we denote as J_{III}. In this point, $V_I = V_s < V_J$. If to lower the position of point J, V_s increases, and V_J decreases. The point where $V_s = V_J$ was denoted as J_{II}.

Let us discuss the case where point I is located above the point 2, and point J is located in between the points J_{II} and J_{III}. The inequality $V_I < V_s < V_J$ takes place. Both c-characteristic lines arrive on the s-shock (Figure 22(b)).

If the c-shock would be located ahead of the s-shock, where $s = s_{\mathrm{I}}$, the velocity of the concentration front would be equal to V_{I}. This is impossible because $V_{\mathrm{I}} < V_{\mathrm{s}}$.

If the c-shock would be located behind the s-shock, where $s = s_{\mathrm{J}}$, the velocity of the concentration front would be equal to V_{J}. This is impossible because $V_{\mathrm{s}} < V_{\mathrm{J}}$.

So there is just one possibility left, which is $V_{\mathrm{c}} = V_{\mathrm{s}}$, saturation and concentration fronts coincide.

Let us find concentration of gas in ganglia behind the displacement front and determine the recovery factor. Substituting values of s and c ahead and behind the displacement front into the condition (17) of the mass balance of gas on the shock, we obtain

$$c_{\mathrm{t}}^{-} = \frac{f_{\mathrm{J}}/(V_{\mathrm{s}} - s_{\mathrm{aJ}})}{s_{\mathrm{J}} - s_{\mathrm{aJ}}} \tag{18}$$

Let us prolong the line I–J until the intersection with the line $f = 0$ at the point $\mathrm{O_D}$ on the plane (s, f) (Figure 22(a)). The numerator in the ratio (18) equals to the length of the interval $\mathrm{O_D}$–$\mathrm{O_J}$, the denominator equals to the length of the interval O–$\mathrm{O_J}$. The interval $\mathrm{O_D}$–$\mathrm{O_J}$ is just a part of the interval O–$\mathrm{O_J}$, so their ratio is less than unity, and $s_{\mathrm{t}}^{-} < 1$.

The saturation decreases on the shock, so some ganglia appear. Concentration jump happens simultaneously with the saturation jump, so it is not clear which concentration of gas c^* is 'carried' by the ganglia which appear from the active phase. The amount of gas which moves into ganglia during the passing of shock front is $c^*(s_{\mathrm{tI}} - s_{\mathrm{tJ}})$, this amount of gas is dissolved in the ganglia behind the displacement front with the saturation s_{tJ}.

Concentration of gas in the 'new' grey ganglia is:

$$c_{\mathrm{t}}^{-} s_{\mathrm{tJ}} = c^*(s_{\mathrm{I}} - s_{\mathrm{J}}), \quad c^* = \frac{f_{\mathrm{J}}/(V_{\mathrm{s}} - s_{\mathrm{aJ}})}{s_{\mathrm{tJ}} - s_{\mathrm{tI}}} \tag{19}$$

The concentration c^* equals to the ratio of segments $\mathrm{O_D}$–$\mathrm{O_J}$ and $\mathrm{O_I}$–$\mathrm{O_J}$. For the case $V_{\mathrm{I}} < V_{\mathrm{s}} < V_{\mathrm{J}}$ the segment $\mathrm{O_I}$–$\mathrm{O_J}$ is longer than the segment $\mathrm{O_D}$–$\mathrm{O_J}$, so the concentration c^* is lower than unity.

The schematic for phases after passing the s–c-shock is shown in Figure 22(d). The ganglia which disjoin the active phase after passing the imbibition shock are grey, the concentration equals to c^*, (19). The average concentration in ganglia is c_{t}^{-}.

So, the residual oleic phase saturation after WAG with intermediate water velocity equals to s_{tJ}, concentration of gas-condensate component in the residual phase equals to $1 - c_{\mathrm{t}}^{-}$. The amount of residual gas-condensate equals $s_{\mathrm{J}} - f_{\mathrm{J}}/V_{\mathrm{s}}$ which is equal to the length of segment O–$\mathrm{O_J}$ (Figure 22(a)).

3.3.3. *White Disjoining Ganglia*

Now let us discuss the case where the point J is between the points $\mathrm{J_{III}}$ and I, and point I is located above the point 2 (Figure 23(a)). For this case the inequality

$V_s < V_I < V_J$ is fulfilled. The concentration front moves ahead of the saturation front with the velocity V_I. Concentration and saturation profiles are shown in Figure 23(c).

Let us find concentration of gas in ganglia after WAG. There is no separation of ganglia on the concentration front because saturation is constant on this shock, so there is no way to change concentration c_t on the concentration jump. This conclusion can also be checked from the condition of gas mass balance on the shock (17). The amount of ganglia which appear on the s-shock is $s_{tI} - s_{tJ}$. Ganglia separate from the active phase which consists on gas only, so the new ganglia also consist on the pure gas (i.e. they are white, Figure 23(d)). The amount of gas which disjoin ganglia is dissolved in the amount of ganglia s_{tJ} behind the s-front. So the concentration c_t^- of gas in the residual ganglia is

$$c_t^- = \frac{s_{tJ} - s_{tI}}{s_{tJ}} \tag{20}$$

After passing the concentration front, gas-condensate is completely displaced by gas from the active phase (Figure 23(d), moment t_2). Therefore, after passing the imbibition saturation front these are gas ganglia which disjoin the active phase (moment t_3). The amount of residual gas-condensate equals the concentration of gas-condensate in the residual ganglia $1 - c_t^-$ times saturation of trapped phase s_{tJ}, as it follows from (20) this amount equals to s_{tI}.

The plot for residual gas-condensate (which is the saturation of residual oleic phase times concentration of gas-condensate in it) versus fractional flow ratio for cases where initial point I is located much higher than the inflection point of the fractional flow curve (Figures 22 and 23) is given in Figure 24. The drainage part of the curve (to the right to point I) corresponds to formula (16). The horizontal segment of imbibition curve corresponds to the case of delayed saturation front where the residual gas-condensate equals the trapped gas-condensate ganglia before the injection, so for the regime shown in Figure 23 the residual gas-condensate is independent on WAG-ratio. For lower values of fractional flow value where the displacement regime transforms to the regime with the single front (Figure 22) the residual gas-condensate is determined by formula (19). For very lower values of fractional flow, which are near to zero, the regime transforms to the regime with advanced saturation front, and residual gas-condensate is determined by (16).

For the case with fast concentration front (Figures 22 and 23), the residual gas-condensate also tends to the value of residual gas-condensate after waterflooding when fractional flow value f^0 tends to zero. For this case the traditional model also predicts zero residual gas-condensate after WAG with any WAG-ratio (Lake, 1989; Bedrikovetsky, 1993).

So, for the miscible WAG with drainage the residual oleic phase saturation equals to the saturation of the trapped ganglia which correspond to the overall oleic phase saturation in the injected gas–water mixture.

For the case of the delayed concentration front, there is no gas dissolved in the trapped gas-condensate. It corresponds to the displacement of gas-condensate–

water mixture with the middle and high water saturation by WAG with the middle and high water–gas ratio.

For the case of the advanced concentration front, gas concentration in the trapped ganglia equals the ratio between the variation of ganglia saturation on the s-shock and the ganglia saturation behind the s-shock, see (20). This case corresponds to displacement of gas-condensate and water with low water–gas-condensate ratio by WAG with low water–gas ratio.

For the intermediate case of the displacement of gas-condensate with low water saturation by WAG with the intermediate water–gas ratio positions of saturation front and of concentration front coincide, gas concentration in residual ganglia are given by formula (18).

4. Transport in Porous Media with Different Wettability

The state of each phase in porous media is strongly wettability-dependent. As it was mentioned above, for strongly water-wet porous media the non-wetting residual oil-condensate is mostly in state of isolated ganglia and droplets. The wetting connate water fills concave surfaces and forms thin films, which are immobile and are geometrically linked to the continuous phase; the wetting phase also forms some ganglia which fill finite clusters of thin pores, as analysed in work (Nikolaevskii, 1993).

Generally speaking, discontinuous phases exist for both wetting and non-wetting phases, but for case of strong wettability of porous media by one phase, ganglia of wetting phase can be ignored. So, for water-wet porous media the effect of oil-condensate ganglia is important, in oil-wet porous media the water droplets are to be taken into account (Figure 25).

With chemical flooding where low concentration aqueous solutions of polymers and surfactants are injected, the mass concentration of chemical is usually used (see

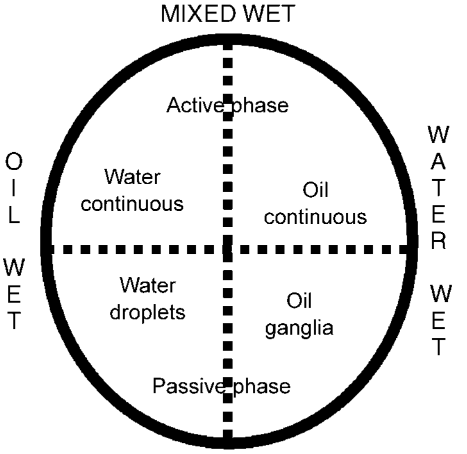

Figure 25. Continuous and discontinuous phases for porous media with different wettability.

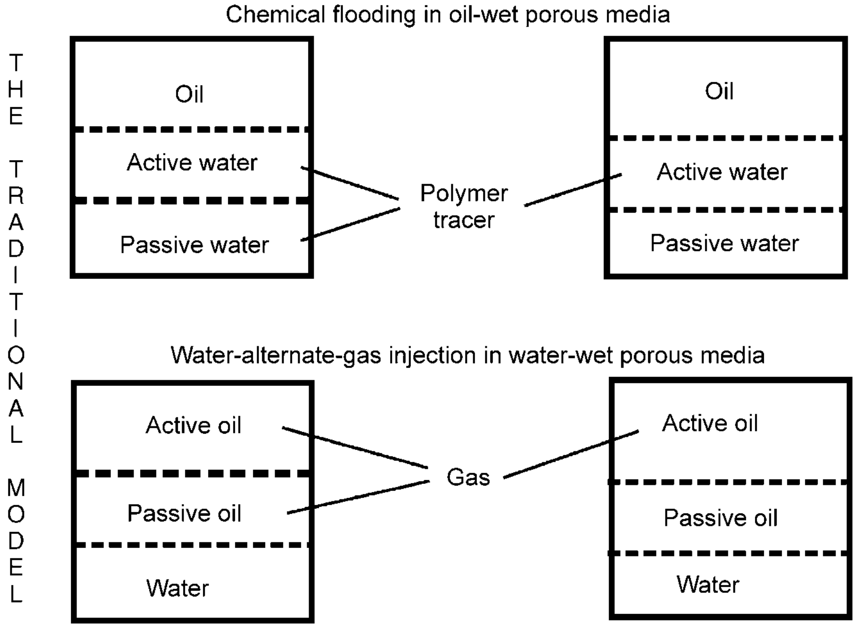

Figure 26. Waterflood with tracer in oil-wet porous media.

Barenblatt and Entov, 1972; Aziz and Settari, 1979; Lake, 1989; Bedrikovetsky, 1993). The injection of an aqueous chemical solution or tracer into oil-wet porous media is also described by Equations (7)–(9) where c and c_t are mass concentrations of chemical in water (Figure 26). Sorption of chemicals can be also handled by adding amounts of adsorbed species in active phase and in ganglia in cumulative terms in mass balance equations (8) and (9).

In the current model (7)–(9) for miscible WAG and gas injection it is assumed that gas injected can be dissolved only in the active oleic phase, while in traditional model gas is assumed to be dissolved in the overall oleic phase (Figure 26). For the process of injection of water with additives into oil-wet porous media (polymer and surfactant flooding, tracer injection) an additive can be dissolved in the active water only, while the conventional equations provide with the additive dissolution in the overall water (Figure 26).

For mixed wet, fraction wet and intermediate wet rocks both phases have active and passive parts (Figure 25). This case is subject of more complex theory.

5. The Model Generalisations and Applications

The equations presented (7)–(9) include effects of different viscosity for injected and displaced gas fluids. The model can be applied for miscible WAG displacement of oil. The analytical 1-D model (14)–(20) was derived for the case where the viscosities of displaced oil-condensate and displacing gas are equal. This model can be applied for cases of low oil-condensate viscosity. Another application is *in situ* gas storage in already waterflooded gas or gas-condensate flied where an annual exploitation cycle includes sequential injection and production of gas, and concentrations of injected and reservoir gases in the produced fluid are to be maintained in strict limits by managing injection and production rates and periods.

The equations presented do not describe viscous fingering. Using the empirical model for an averaged gas component fractional flow and phase mobility in three component flow (Blunt and Christie, 1993) allows to derive a model which account for both viscous fingering and ganglia.

The Equations (7)–(9) ignore dissolution of injected gas in water which is unacceptable for CO_2 floods. The diffusion of CO_2 through the water phase probably plays a major role in the recovery processes, which is controlled by the mass-transfer rate (Mueller and Lake, 1990). Introduction of CO_2 concentration in water and inter phase mass transfer terms allows to study the effects of CO_2 diffusion from mobile gas phase to ganglia through water on oil recovery.

6. Summary

For the case of immiscible displacement the model which honours phase discontinuities coincides with the traditional Buckley-Leverett equation.

6.1.1.1. *Features of the Model with Ganglia.* The model for two phase multicomponent flow honouring phase discontinuities differs significantly from the traditional model. The reason for this difference is: the component, which is insoluble in the wetting phase and is injected together with non-wetting phase, can be dissolved in the active non-wetting phase only, and ganglia are inaccessible for this component. If the discontinuous part of the phase is not considered, as traditional model does, the component is distributed homogeneously in the overall non-wetting phase, which is a simplified image of two-phase multicomponent flow in porous media.

Mechanisms of mass exchange between continuous phase and ganglia are different for imbibition and for drainage. Therefore, the model developed is of a hysteretic type.

6.1.1.2. *Active Saturation Function.* The new equations proposed contain a new empirical function of active phase saturation versus overall saturation. A method for prediction of this function from hysteretic relative permeability curves for non-wetting phase is developed. Calculations using this method show excellent agreement with the data from direct laboratory measurements. It confirms the main assumption of the model that the distribution of non-wetting phase on an active part and on ganglia is determined by the value of saturation.

6.1.1.3. *Effects.* The model proposed predicts faster propagation of the component injected with non-wetting phase than the traditional model. This is due to the fact that the injected component is transported in an active part of the phase with lower saturation rather than in an overall phase with higher saturation.

The proposed model predicts significantly lower recovery factor for miscible WAG injection if compared with the traditional model. This is due to the fact that some gas-condensate is trapped in ganglia state behind the miscible displacement front. It is worth to emphasise that the traditional model predicts no oil-condensate remaining after a miscible flooding.

6.1.1.4. *Structure of Residual Reserves after Miscible WAG.* Analytical solutions for displacement of oil-condensate with water by miscible gas with water exhibit a complex picture of 'active phase–ganglia' mass transfer and of residual oil-condensate distribution after flooding.

If the fractional flow of gas in the injected gas–water mixture is higher than the fractional flow for gas-condensate in the displaced gas-condensate–water fluid, some oil-condensate ganglia join the expanding active oleic phase. The ganglia which do not join active phase remains in porous media after the flooding.

If the fractional flow of gas in the injected gas–water mixture is lower than the fractional flow for oil-condensate in the displaced oil–water fluid, some ganglia disjoin active phase and remain in porous media after the flooding. For the case where the velocity of the saturation front is higher than the velocity of the concentration front, the disjoining ganglia consist of oil-condensate only. For the case where the velocity of the saturation front is lower than the velocity of the concentration front, the disjoining ganglia consist on injected gas only. If the velocity of the saturation front is lower than the velocity of concentration wave which propagates over the injected state but is higher then the velocity of concentration wave which propagates over the initial state, the disjoining ganglia consist on the gas–oil mixture with the concentration which is calculated from the analytical solution.

The oil-condensate ganglia which have been present in porous media before the injection, remain in porous media after application of WAG with imbibition.

6.1.1.5. *Applications.* The model developed describes miscible WAG and gas injection into water-wet reservoirs as well as chemical flooding and tracer injection in oil-wet reservoirs.

If to nominate an initial reservoir fluid as 'oil pseudo component' and an injected gas as 'gas pseudo component', the model presented describes multicomponent displacement for any number of components.

If the component injected is soluble in both phases, it diffuses from active non-wetting phase towards ganglia via the wetting phase. Concentrations of this component in active phase and in ganglia are linked by the kinetic equation, where the delay equals to the time of diffusion.

General theory for 3-phase flows with ganglia is very complex but can be simplified for specific cases. For immiscible WAG we introduce two trapped phases: 'oil in water' and 'oil in gas'. Saturations of trapped phases are functions of saturations of water and gas phases, it closes the system of governing equations.

7. Conclusions

1. The traditional mathematical model for 2-phase multicomponent displacements (EOR) contradicts the conventional image about non-wetting phase in porous media which is present simultaneously as continuous mobile phase and as separated immobile ganglia.
2. A new mathematical model for 2-phase multicomponent flows in porous media which accounts for ganglia and droplets of non-wetting phase has been developed.
3. The new model shows excellent agreement with laboratory experiments while the traditional model significantly overestimates the recovery.
4. The new model shows significant residual oil after miscible WAG while the traditional model predicts no residual oil.

Appendix A. Mass Balance Equations

Equation for continuity of water is:

$$\Phi\frac{\partial\rho_{\mathrm{W}}(1-s)}{\partial t}+\mathrm{div}\rho_{\mathrm{W}}u_{\mathrm{W}}=0 \tag{A.1}$$

Gas and oil-condensate components are present in both active and trapped phases, the transport is going on via the active phase. Therefore, the mass balance equations for gas component and for oil-condensate component in both active and trapped phases are:

$$\frac{\partial}{\partial t}(\rho_{\mathrm{O}}c^{m}s_{\mathrm{a}}+\rho_{\mathrm{O}}c_{\mathrm{t}}^{m}s_{\mathrm{t}})+\mathrm{div}(\rho_{\mathrm{O}}c^{m}u_{\mathrm{O}})=0 \tag{A.2}$$

$$\frac{\partial}{\partial t}(\rho_{\mathrm{O}}(1-c^{m})s_{\mathrm{a}}+\rho_{\mathrm{O}}(1-c_{\mathrm{t}}^{m})s_{\mathrm{t}})+\mathrm{div}(\rho_{\mathrm{O}}(1-c^{\mathrm{m}})u_{\mathrm{O}})=0 \tag{A.3}$$

Mass balance equations for gas component in ganglia and for oil-condensate component in ganglia are:

$$\Phi\frac{\partial\rho_{\mathrm{Ot}}c_{\mathrm{t}}^{m}s_{\mathrm{t}}}{\partial t}=-q_{\mathrm{c}}^{m} \tag{A.4}$$

$$\Phi\frac{\partial\rho_{\mathrm{Ot}}(1-c_{\mathrm{t}}^{m})s_{\mathrm{t}}}{\partial t}=-q_{1-\mathrm{c}}^{m} \tag{A.5}$$

From formula (4) and from the explanation of the influx and of the outflux (Figure 13) we obtain the following expression for terms of interphase mass transfer between active and trapped phases by the gas component q_{c}^{m} and by the oil-condensate component $q_{1-\mathrm{c}}^{m}$

$$\begin{aligned} q_{\mathrm{c}}^{m} &= c_{\mathrm{t}}^{m}\rho_{\mathrm{Ot}}q, \quad q_{1-\mathrm{c}}^{m}=(1-c_{\mathrm{t}}^{m})\rho_{\mathrm{Ot}}q, \quad \frac{\partial s}{\partial T}>0 \\ q_{\mathrm{c}}^{m} &= c^{m}\rho_{\mathrm{Oa}}q, \quad q_{1-\mathrm{c}}^{m}=(1-c^{m})\rho_{\mathrm{Oa}}q, \quad \frac{\partial s}{\partial T}<0 \end{aligned} \tag{A.6}$$

Substituting the expression for the volumetric exchange term (4) into mass exchange terms (A.6) we obtain equation for mass balance of gas component in the trapped phase:

$$\begin{aligned}\frac{\partial \rho_{\mathrm{Ot}} c_{\mathrm{t}}^{m} s_{\mathrm{t}}}{\partial t} &= \rho_{\mathrm{Ot}} c_{\mathrm{t}}^{m} \frac{\partial s_{\mathrm{t}}}{\partial t}, \quad \frac{\partial s}{\partial t} < 0 \\ \frac{\partial \rho_{\mathrm{Ot}} c_{\mathrm{t}}^{m} s_{\mathrm{t}}}{\partial t} &= \rho_{\mathrm{Oa}} c^{m} \frac{\partial s_{\mathrm{t}}}{\partial t}, \quad \frac{\partial s}{\partial t} > 0 \end{aligned} \tag{A.7}$$

Appendix B. Closed System of Governing Equations

From the dependence $s_{\mathrm{a}}(s)$ follows that relative permeabilities for mobile phases are functions of s and c^{m}:

$$u_{\mathrm{j}} = -k \frac{k_{\mathrm{rj}}(s_{\mathrm{a}}, s, c^{m})}{\mu_{\mathrm{j}}(c^{\mathrm{m}})} \nabla p, \quad \mathrm{j} = \mathrm{W}, \mathrm{O} \tag{B.1}$$

Therefore, fractional flow is also the function of s and c^{m}:

$$u_{\mathrm{O}} = fU; \quad u_{\mathrm{W}} = (1 - f)U; \quad U = u_{\mathrm{O}} + u_{\mathrm{W}} \tag{B.2}$$

Adding two equations (B.1) we obtain expression for the total flux of two-phase fluid

$$U = -k\lambda(s, c^{m}) \nabla p \tag{B.3}$$

$$\lambda(s, c) = \frac{k_{\mathrm{rO}}(s_{\mathrm{a}}(s), s, c^{m})}{\mu_{\mathrm{O}}(c^{m})} + \frac{k_{\mathrm{rW}}(s_{\mathrm{a}}(s), s, c^{\mathrm{m}})}{\mu_{\mathrm{W}}} \tag{B.4}$$

Equations (A.1)–(A.5), (A.7) and (B.1)–(B.4) form a closed system of governing equations for two-phase three-component flow in porous media honouring ganglia of non-wetting phase.

Substitution of the modified Darcy's law (B.1) into Equations (A.1)–(A.5) and (A.7) allows to obtain four governing equations, the unknowns are p, s, c^{m} and c_{t}^{m}.

Equation for volumetric balance of water follows from (A.1) and (B.1)–(B.3) with the assumption of water incompressibility:

$$-\Phi \frac{\partial s}{\partial t} = \mathrm{div}((1 - f)\lambda(s, c^{m}) \nabla p) \tag{B.5}$$

Equations for mass balance of gas and oil-condensate components in the overall oleic phase follows from (A.2), (A.3) and (B.1)–(B.3):

$$\Phi \frac{\partial}{\partial t}(\rho_{\mathrm{O}} c^{m} s_{\mathrm{a}} + \rho_{\mathrm{O}} c_{\mathrm{t}}^{m} s_{\mathrm{t}}) = \mathrm{div}(\rho_{\mathrm{O}} c^{\mathrm{m}} f(s, c) \lambda(s, c) \nabla p) \tag{B.6}$$

$$\Phi \frac{\partial}{\partial t}(\rho_{\mathrm{O}}(1 - c^{m}) s_{\mathrm{a}} + \rho_{\mathrm{O}}(1 - c_{\mathrm{t}}^{m}) s_{\mathrm{t}}) = \mathrm{div}(\rho_{\mathrm{O}}(1 - c^{m})(1 - f)\lambda(s, c) \nabla p) \tag{B.7}$$

Equations (A.7) and (B.5)–(B.7) form the closed system of governing equations.

The traditional equations can be obtained from the system derived by just assuming $s_{\mathrm{t}} = 0$. Equations (B.5)–(B.7) with $s_{\mathrm{t}} = 0$ and $s_{\mathrm{a}} = s$ describe two-phase three-component flow in porous media without considering ganglia (Aziz and Settari, 1979; Lake, 1989; Bedrikovetsky, 1993) and determine unknowns p, s and c^m.

Appendix C. Initial and Boundary Conditions for 3-D Reservoir Model

Initial conditions are:

$$t = 0: \quad s = s_{\mathrm{I}}(x), \quad c^m = c^m_{\mathrm{I}}(x), \quad c^m_{\mathrm{t}} = c^m_{\mathrm{tI}}(x), \quad x \in D \tag{C.1}$$

The system (A.7) and (B.5)–(B.7) is elliptic for the pressure $p(x, t)$ (the detailed mathematical analysis of analogous problem for two-phase flow of incompressible fluids can be found in Antontsev *et al.* (1990) and Mitlin (1993)), so initial conditions for pressure are not to be prescribed.

We introduce surfaces of injection wells Γ^+ and of production wells Γ^- inside three-dimensional domain D.

Boundary conditions on the injection wells surface Γ^+ are:

$$x \in \Gamma^+: \quad p = p^0(x, t), \quad f = f^0(x, t), \quad c^m = c^{m0}(x, t) \tag{C.2}$$

For conservation laws (B.5)–(B.7) three fluxes for water, gas and gas-condensate are to be posed on the injection surface Γ^+. The water flux is determined by the fraction f and by the velocity U, together with gas concentration c^m it determine fluxes of gas component and of oil-condensate component.

Although often in the literature the water saturation s is set on the injection surface instead of the water flux f, this formulation can result in the unsolvable singularity in the neighbourhood of the injection surface (the example is shown in Barenblatt and Entov (1972)), so setting the saturation value on the injection surface Γ^+ results in an ill-posed problem.

The unknown concentration c^m_{t} is ‘attached’ to the immobile phase and is not transferred by any flux. Therefore, the problem for the function c^m_{t} is of Goursat type (Tikhonov and Samarsky, 1963). So, the initial condition for c^m_{t} is to be posed, the boundary condition for c^m_{t} on the injection surface is not to be set because there is no flux of components in ganglia. The analogous case for non-equilibrium sorption was analysed in Fishlock *et al.* (1988), Bedrikovetsky (1993).

The boundary condition on the production surface Γ^- is:

$$x \in \Gamma^-: \quad p = p^-(x) \tag{C.3}$$

The system (A.7) and (B.5)–(B.7) is hyperbolic for saturation s and for concentration c^m, so initial conditions for these two unknowns are to be set, and boundary conditions for them are to be posed on the injection surface Γ^+ only (the detailed analysis for analogous problem for two-phase multicomponent flow is given in Antontsev *et al.* (1990) and Mitlin (1993)).

Condition of impermeability is posed on the boundary of the flow domain:

$$x \in \partial \mathrm{D}: \quad (\nabla p)_n = 0 \tag{C.4}$$

The problem (C.1)–(C.4) is properly posed if the pressure gradient on the injection surface is not tangent to this surface.

Appendix D. Stability of Concentration Shock

Stability of c-shocks with respect to vanishing smoothing is proven by construction of the solution of the initial-value problem with the smoothed jumps. c-characteristic lines for the solution obtained are shown in Figures 20–23(b). With the smoothing interval tending to zero, the continuous solution tends to the initial shock.

Acknowledgements

Many thanks to colleagues from PETROBRAS: to Mr Gersem M. Andrade and Mr Walter Lemos Pedrone for critical comments; to Dr Eraldo Luiz Ferreira, Dr Jose Roberto P. Rodrigues and Mr Carlos Holleben for useful discussions; to Mr Gersem M. Andrade and Prof Dan Marchesin for help with the preparing of the manuscript; to Prof Euclides Bonet for providing the experimental paper which enables the verification of the theory developed; to Dr Paolo Roberto Ballin who is constantly encouraging this work. Special gratitude is to be expressed to Dr A. Shapiro and Prof E. Stenby (Denmark Technical University) and Prof V. I. Maron (Moscow Gas-condensate and Gas Academy, Russia) for discussion the basics of the theory. Especial gratitude is due to Prof. L.W. Lake (Texas University at Austin) for the text revision and editing.

References

Antontsev, S. N., Kazhikhov, A. V. and Monakhov, V. N.: 1990, *Boundary-Value Problems in Mechanics of Nonhomogeneous Fluids, Studies in Mathematics and Its Applications*, Vol. 22, North-Holland, Amsterdam.

Aziz, K. and Settari, A.: 1979, *Petroleum Reservoir Simulation*, Applied Science Publishers, London.

Barenblatt, G. I. and Entov, V. M.: 1972, Non-equilibrium phenomena in the flow of immiscible fluids in porous media, in: *Numerical Methods of Solution of Problems of Flow of Multiphase Incompressible Fluids in Porous Media*, Novosibirsk, Russia, (in Russian).

Barenblatt, G. I., Entov, V. M. and Rizhik, V. M.: 1987, *Theory of Fluid Flows through Natural Rocks*, Kluwer Academic Publishers, London/Boston/Dordrecht.

Bedrikovetsky, P. G.: 1993, *Mathematical Theory of Oil and Gas Recovery*, Kluwer Academic Publishers, London/Boston/Dordrecht.

Blunt, M. and Christie, M.: 1993, How to predict viscous fingering in three component flow, *Transport Porous Med.* **12**, 207–236.

Campbell, B. T. and Orr Jr., F. M.: 1985, Flow visualisation for CO2/Crude oil displacements, *SPEJ*, 665–678.

Carson, L. D.: 1989, Waterflooding increases gas recovery, *JPT*.

Caudle, B. H. and Dyes, A. B.: 1958, Improving miscible displacement by gas–water injection, *Trans. AIME* **213**, 281–291.

Chartsis, J., Morrow, N. R. and Lim, H. T.: 1983, Magnitude and detailed structure of residual oil saturation, *SPEJ* **23**, 2.

Cullick, A. S., Lu, H. S., Jones, L. G., Cohen, M. F. and Watson, J. P.: 1993, WAG may improve gas-condensate recovery, *SPE RE*, 207–213.

Dullien, F. A. L.: 1992, *Porous Media: Fluid Transport and Pore Structure*, 2nd edn., Academic Press Inc., NY/Boston/London.

Fishlock, et al., T. P.: 1988, Experimental studies on the waterflooding residual gas saturation and its production by blowdown, *SPE RE*, 387–397.

Green, D. W. and Willhite, G. P.: 1998, *Enhanced Oil Recovery*, SPE Textbook Series, Robertson, TX.

Hawes, et al., R. I.: 1986, Feasibility studies of waterflooding gas-condensate reservoirs, SPE Paper 15875 presented at the 1986 European Petroleum Conference, London, October 1986, 20–22.

Henderson, G. D., Danesh, A. S. and Peden, J. M.: 1991a, Experimental investigation of waterflooding gas-condensate reservoirs and their subsequent blowdown, European Symposium on IOR, Stavanger, Norway.

Henderson, G. D., Danesh, A. S. and Peden, J. M.: 1991b, Waterflooding of gas-condensate fluids in cores abeve and below the dewpoint, SPE Paper 22636 presented at 66th Annual Technical Conference and Exhibition of SPE, Dallas, TX, October 1991, 6–9.

Lake, L. W.: 1989, *Enhanced Oil Recovery*, Prentice-Hall, Englewood Cliffs, New Jersey.

Mitlin, V.: 1993, *Non-Linear Dynamics of Reservoir Mixtures*, CRC Press, Boca Raton/SLA, 257 pp.

Mueller, T. and Lake, L. W.: 1990, A theoretical study of waterblocking in miscible flooding. SPE Paper 20206 presented at 7th SPE/DOE Symposium on Enhanced Oil Recovery, Tulsa, OK, April 22–25, 1990.

Nikolaevskii, V. N.: 1993, Theory of the vibration in oil reservoirs, In: *Vibration in Oil Fields*, Russian Academy of Sciences, Moscow.

Raimondi, P. and Torcaso, M. A.: 1964, Distribution of the oil phase obtained upon imbibition of water, *SPEJ*.

Seljakov, V. I. and Kadet, V. V.: 1997, *Percolation Theory of Transport in Porous Media*, Kluwer Academic Publishers, London/Boston/Dordrecht.

Shelton, J. L. and Schneider, F. N.: 1975, The effects of water injection on miscible flooding methods using hydrocarbons and carbon dioxide, *SPEJ*, 217–226.

Stalkup Jr., F. I.: 1970, Displacement of oil by solvent at high water saturation, *SPEJ*, 337–348.

Stalkup Jr., F. I.: 1983, *Miscible Displacement*, Monograph Series 8, SPE, Richardson, TX.

Stauffer, D. and Aharony, A.: 1992, *Introduction in Percolation Theory*, Taylor & Francis, London/Washington.

Ter-Sarkisov, R. M.: 1995, *Enhanced Hydrocarbon Recovery of Oil-Gas-Condensate Reservoirs*, Nedra, Moscow.

Tiffin, D. L. and Yellig, W. F.: 1983, Effects of mobile water on multiple-contact miscible gas displacement, *SPEJ*, 447–455.

Tiffin, D. L., Sebastian H. M. and Bergman, D. F.: 1991, Displacement mechanism and water shielding phenomena for a rich-gas/crude-oil system, *SPERE*, 193–199.

Tikhonov, A. N. and Samarsky, A. A.: 1963, *Equations on Mathematical Physics*, International Series of Monographs on Pure and Applied Mathematics, Vol. 39, Pergamon Press, London.

Todd, M. R., Cobb W. M. and McCarter, D. E.: 1982, CO_2 flood performance evaluation for the Cornell Unit, Wasson San Andres Field, JPT, October 1982, 2271–2282.

Walsh, M. P. and Lake, L. W.: 1989, Applying fractional flow theory to solvent flooding and chase fluids, *J. Petrol. Sci. Eng*. **2**, 281–303.

Zakirov, S. N. and Shandrigin, A.: 1988, WAG flood of gas-condensates, USSR Academy of Sciences, Institute for Oil and Gas Problems (IPNG), Moscow, Russia (in Russian).